

Quantum chaos and its observation in coupled optical solitons

A. P. Alodjants and S. M. Arakelian

Vladimir State Technical University, 600026 Vladimir, Russia

(Submitted 30 May 1994)

Zh. Éksp. Teor. Fiz. **107**, 1792–1825 (June 1995)

We examine various problems involving the transition of a nonlinear interaction to chaos under energy exchange between two modes in a quantum system with distributed feedback. Our principal emphasis is on clarification of the structure of the emergent chaos, the feasibility of controlling that chaos, and the experimental measurement procedure appropriate to an actual quantum system. We write down the fundamental relations and the basic equations; to solve the latter we use quantum perturbation theory for two-soliton states in the semiclassical approximation. The basic nonclassical effects in these states are discussed, the major ones being the onset of quantum chaos and methods of controlling it for solitons in tunnel-coupled optical fibers. The feasibility of experimentally verifying this fundamental state in such a system is related to the problem of making quantum nondemolition measurements of photon numbers in the coupled-soliton problem. © 1995 American Institute of Physics.

1. INTRODUCTION

Notwithstanding a great deal of work having been devoted to the quantum properties of optical solitons (see, e.g., Ref. 1 and the recent Refs. 2–4), a number of problems related to the generation of quantum coupled soliton states remain open, both from a practical and a more fundamental standpoint.

Indeed, the elucidation of the physics and the conditions under which quantum coupled solitons are produced has fueled some hope of applying them to optical information processing in multichannel communications systems. On the other hand, the actual physics of soliton wave packet behavior is an interesting optics problem in its own right, since it may lead to new, nontrivial effects.

From a quantum point of view, we are dealing with the possible occurrence of optical wave packets with sub-Poisson statistics, the feasibility of quantum nondemolition measurements, and the production of light (solitons) in a quadrature squeezed state.^{2,3} Furthermore, analysis of the classical problem shows that the behavior of soliton-like entities in nonintegrable systems can be so complicated that stochastic dynamics and chaos ensue (as manifested in the parameters of these quasisolitons).⁵

Although it is well known that the nonlinear Schrödinger equation with periodic boundary conditions is completely integrable (a fact we make use of in the present paper; see Ref. 5, for example), the use of approximate analytical methods in modeling (as in the nonlinear oscillator example, for instance) and allowance for losses are of interest in their own right, and can lead to instabilities.

Discussion of the analogs of these phenomena in quantum theory, therefore, is essentially a new problem in quantum optics (cf. Ref. 6). That problem is examined in the present paper as it applies to two interacting solitons in a special type of optical fiber with efficient energy exchange between modes.

In the simplest case, the quantum theory of two-soliton states is presented, for example, in the seminal paper by Za-

kharov and Shabat.⁷ The approach developed in that paper, however, does not deal with the actual interaction between the solitons, merely assuming that they are infinitely far apart when the interaction begins and ends. Taking the same approach, it has even been shown³ that quantum nondemolition measurements are feasible when both solitons possess appropriate integrals of the motion, specifically the number of photons and momentum.

Here we develop a different approach that we believe better captures the physics of the problem, and takes the details of the interaction into account. We solve the problem in the adiabatic approximation of perturbation theory,⁸ detailing three possible scenarios: Two-soliton states of interest (higher-order solitons) are produced in a conventional nonlinear optical fiber. Coupled soliton states are produced in a special type of optical fiber—one with two tunnel-coupled strands—due to efficient (linear) energy exchange between the modes propagating in the fiber strands. Intrinsic two-soliton states are produced in each of two tunnel-coupled strands of such a fiber. In this last case we have a four-body problem (two solitons in each channel).

We employ the Hartree approximation in the Schrödinger representation for the quantum calculations in this problem. The usefulness of this approach in such problems (see Refs. 3 and 9, for example) stems from its generality and the simple physical interpretation of results that it provides, which facilitates comparison with classical analogs.

Rather than going directly to our original results, we point out that the class of equations that engenders the soliton solutions we consider here have the nonlinear Schrödinger equation as their archetype. These equations have appeared in various forms, however. They are discussed in Refs. 10–12, and we relate them to the present problem in Appendix 1, where we actually justify the validity of our approach.

The paper is organized as follows. Section 2 lists the basic relations and equations. Quantum perturbation theory is developed for two-soliton states in Sec. 3. The major nonclassical effects for these states are discussed in Sec. 4. Sec-

tion 5—the heart of the paper—details the emergence and control of quantum chaos in tunnel-coupled optical fibers. The main conclusions are summarized at the end of the paper. Two appendices address collateral questions that are important to an understanding of the central problem; in particular, Appendix 2 provides calculations of quantum nondemolition measurements of the number of photons in the coupled-soliton problem.

2. BASIC RELATIONS

In the Schrödinger picture in tunnel-coupled optical fibers, the propagation and interaction of two solitons (which we denote by 0 and h) can be described by the Hamiltonian

$$H = \hbar \sum_{i,j} \left\{ \frac{1}{2} \int_{-\infty}^{\infty} a_{ix}^+(x) a_{ix}(x) dx - \frac{\kappa}{2} \int_{-\infty}^{\infty} [a_i^+(x)]^2 a_i^2(x) dx + \varepsilon \int_{-\infty}^{\infty} a_i^+(x) a_j(x) dx \right\}, \quad (1)$$

$$i, j = 0, h, \quad i \neq j,$$

where the first term on the right-hand side accounts for the dispersive medium, the second accounts for the cubic nonlinearity ($\kappa \sim \chi^{(3)}$) responsible for the interaction, and the third describes the soliton interaction (we specify the coupling constant ε below). Operators $a_i(x)$ and $a_i^+(x)$ ($i=0, h$) are annihilation and creation operators, respectively, which obey the commutation relations for a Bose-Einstein system:

$$[a_i(x); a_j^+(x')] = \delta_{ij} \delta(x-x'), \quad (2a)$$

$$[a_i(x); a_i(x)] = [a_i^+(x); a_i^+(x)] = 0, \quad (2b)$$

$$i, j = 0, h.$$

We seek a system state vector $|\xi\rangle$ in the Schrödinger picture in the form³

$$|\xi\rangle = \sum_{n,m} w_{nm} \int_{-\infty}^{\infty} f_{nm}(x_1 \dots x_n, x_{n+1} \dots x_m, t) \times \prod_{i=1}^n a_0^+(x_i) \prod_{j=1}^m a_h^+(x_j) dx_i dx_j |0\rangle, \quad (3)$$

where the function f_{nm} is defined in (6). The state vector satisfies the Schrödinger equation:

$$i\hbar \frac{d}{dt} |\xi\rangle = H |\xi\rangle. \quad (4)$$

Here t is the longitudinal coordinate for soliton propagation; in quantum theory, this is the time.^{9,10,12} Note that in the Heisenberg picture, all of the operators introduced thus far are functions of time, so we obtain the familiar quantum Schrödinger equation for the $a_i(t, x)$ (see below).

The quantities w_{nm} are responsible for the initial ($t=0$) photon distribution (which we assume to be Poisson), i.e., the light is in a coherent state at $t=0$. Then

$$w_{nm} = w_n w_m = \exp[-0.5(|\alpha_{01}|^2 + |\alpha_{02}|^2)] \frac{\alpha_1^n \alpha_2^m}{\sqrt{n!m!}} \quad (5)$$

where $|\alpha_{01}|^2$ and $|\alpha_{02}|^2$ are the respective initial mean photon numbers in the two modes (0 and h).

With the interaction Hamiltonian (1), we proceed to solve this problem in the Hartree approximation. We assume that

$$f_{nm} = f_n f_m = \prod_{i=1}^n \prod_{j=n+1}^m \Psi_n^{(1)}(x_i, t) \Psi_{m+n}^2(x_j, t), \quad (6)$$

where $\Psi_n^{(1)}$ and $\Psi_{m+n}^{(2)}$ are the desired wave functions for the 0 and h solitons, with the normalization

$$\int_{-\infty}^{\infty} |\Psi_{n,m+n}^{(1,2)}(x_i, t)| dx = 1. \quad (7)$$

Plugging (5) and (6) into the Schrödinger equation (4), we obtain

$$\begin{aligned} & i \prod_{i=1}^n \prod_{j=n+1}^m \frac{\partial}{\partial t} [\Psi_n^{(1)}(x_i, t) \Psi_{n+m}^{(2)}(x_j, t)] \\ &= - \prod_{j=n+1}^{n+m} \Psi_{n+m}^{(2)}(x_j, t) \sum_{i=1}^n \frac{\partial^2}{\partial x_i^2} \prod_{i=1}^n \Psi_n^{(1)}(x_i, t) - \prod_{i=1}^n \Psi_n^{(1)} \\ & \quad \times (x_i, t) \sum_{j=n+i}^{n+m} \frac{\partial^2}{\partial x_j^2} \prod_{j=n+1}^{n+m} \Psi_{n+m}^{(2)}(x_j, t) \\ & \quad - 2\kappa \left\{ \prod_{j=n+1}^{n+m} \Psi_{n+m}^{(2)}(x_j, t) + \sum_{1 \leq i < k \leq n} \delta(x_k - x_i) \right. \\ & \quad \times \prod_{i=1}^n \Psi_n^{(1)}(x_i, t) + \prod_{i=1}^n \Psi_n^{(1)}(x_i, t) \\ & \quad \times \left. \sum_{1+n \leq j < k \leq n+m} \delta(x_k - x_j) \prod_{j=n+1}^{m+n} \Psi_{m+n}^{(2)}(x_j, t) \right\} \\ & \quad + \varepsilon \left\{ n \prod_{i=1}^{n-1} \Psi_n^{(1)}(x_i, t) \prod_{j=n}^{n+m} \Psi_{n+m}^{(2)}(x_j, t) \right. \\ & \quad \left. + m \prod_{i=1}^{n+1} \prod_{j=n+2}^{n+m} \Psi_{n+m}^{(2)}(x_j, t) \Psi_n^{(1)}(x_i, t) \right\}. \quad (8) \end{aligned}$$

Equation (8) can be interpreted physically in terms of a Bose gas model in which “two types” of particles interact. Specifically, terms with derivatives $\partial^2/\partial x_i^2$ correspond to the kinetic energy of types 0 and h bosons; the term with coefficient 2κ describes a delta-function interaction among these same 0 and h modes; and the last term describes the interaction between the 0 and h modes.

Subsequent calculations are similar to those used in Ref. 3. We multiply Eq. (8) on the left by f_{nm}^* and integrate over all $\prod_{i=1}^n dx_i \prod_{j=n+1}^{n+m} dx_j$. We ultimately obtain a certain functional, which when varied yields a system of equations for $\Psi_{n,n+m}^{(1,2)}(x, t)$:

$$\begin{aligned}
i \frac{\partial}{\partial t} \Psi_n^{(1)} &= -\frac{\partial^2}{\partial x^2} \Psi_n^{(1)} - 2(n-1)\kappa |\Psi_n^{(1)}|^2 \Psi_n^{(1)} + \varepsilon \Psi_{n+m}^{(2)}, \\
i \frac{\partial}{\partial t} \Psi_{n+m}^{(2)} &= -\frac{\partial^2}{\partial x^2} \Psi_{n+m}^{(2)} - 2(m-1)\kappa |\Psi_{n+m}^{(2)}|^2 \Psi_{n+m}^{(2)} \\
&\quad + \varepsilon \Psi_n^{(1)}.
\end{aligned} \tag{9}$$

The equations (9) for the wave functions (c numbers) of the interacting solitons can be brought into correspondence with the classical coupled nonlinear Schrödinger equations that describe the propagation of optical wave packets in tunnel-coupled fibers by specifying the meaning of the variables t and x . In the classical nonlinear Schrödinger equations for optical solitons, t [which we take to be the time, as in quantum mechanics; see Eq. (4)] is the longitudinal coordinate with regard to soliton propagation, and x is either the dynamical coordinate (see Appendix 1 and Ref. 5) or the translational coordinate of the center of mass, which moves with group velocity $v_{gr} = 1/k'$.³ In the latter case, $t = k''z/2|k'|^2$, $x = v_{gr}\tau - z$, and $\kappa = \tilde{\chi}|k'|^2 I^2/k''$ ($\tilde{\chi}$ accounts for the Kerr nonlinearity, I is a mean (or initial) normalized intensity measurement, and k'' specifies the group velocity dispersion to second order³). The equations (9) then correspond to Eq. (A2) of Appendix 1.

The parameters $t_{NL,n} \sim 1/n\kappa$ and $t_{NL,m} \sim 1/m\kappa$ are the characteristic phase modulation time scales (which determine the corresponding spatial scales) for either soliton; $t_b \sim 1/\varepsilon$ is the characteristic "linear" beat period between the two channels (see Ref. 13), and ε actually specifies the interaction within the system.

In our previous paper,⁹ we assumed that $t_{NL,n}, t_{NL,m} > t_b$. Here, we propose instead a perturbation solution of (9) for solitons in the adiabatic approximation,⁵ and assume that $t_b \gg t_{NL,n}, t_{NL,m}$. In addition, we take $m \sim n \gg 1$. Normalizing t with a factor of 2 and setting

$$\Phi_{n,n+m}^{(1,2)} \equiv \sqrt{n\kappa} \Psi_{n,n+m}^{(1,2)}, \tag{10}$$

we obtain

$$\begin{aligned}
i \frac{\partial}{\partial t} \Phi_n^{(1)} &= -\frac{1}{2} \frac{\partial^2}{\partial x^2} \Phi_n^{(1)} - |\Phi_n^{(1)}|^2 \Phi_n^{(1)} + \varepsilon' \Phi_k^{(2)}, \\
i \frac{\partial}{\partial t} \Phi_k^{(2)} &= -\frac{1}{2} \frac{\partial^2}{\partial x^2} \Phi_k^{(2)} - |\Phi_k^{(2)}|^2 \Phi_k^{(2)} + \varepsilon' \Phi_n^{(1)},
\end{aligned} \tag{11}$$

where $k \equiv n+m$ and $\varepsilon' \equiv \varepsilon/2$ (as before, we denote the normalized value of t by the same symbol for the sake of brevity).

We are presently most interested in two-soliton coupled states in the two-channel system (11). It is therefore worthwhile to consider two-soliton states in each channel individually. This problem, which we analyze in the next section, has much in common with that of the fundamental solitons described by (11).

3. QUANTUM PERTURBATION THEORY FOR TWO-SOLITON STATES. ANALYTICAL METHOD

For two weakly coupled channels ($\varepsilon' \approx 0$), Eqs. (11) become independent, as do the two-soliton states produced in

each strand of the optical fiber. It is therefore sufficient to consider the formation of coupled second-order solitons, in the 0 channel, for example, which are described by the wave function $\Psi_n^{(1)}$.

On the other hand, we can make use of the general theory of two-soliton quantum states (denoted by subscripts $n_{1,2}$) in the Hartree approximation.³ The wave function then takes the form

$$\Psi_{n_1 n_2}^{(1)} = \sqrt{\frac{n_1}{n_1+n_2}} \Psi_{n_1}^{(1)} + \sqrt{\frac{n_2}{n_1+n_2}} \Psi_{n_2}^{(1)}. \tag{12}$$

Here n_1 and n_2 give the number of photons in the two solitons produced in the 0 channel ($n_1+n_2=n$) and described by the wave functions $\Psi_{n_1}^{(1)}$ and $\Psi_{n_2}^{(1)}$. Physically, Eq. (12) describes well-separated solitons. The equations for $\Psi_{n_1 n_2}^{(1)}$ can be derived (in the Hartree approximation) by minimizing a functional (with $\varepsilon' = 0$)³; they take the form

$$\begin{aligned}
i \frac{\partial}{\partial t} \Psi_{n_1 n_2}^{(1)} &= -\frac{\partial^2}{\partial x^2} \Psi_{n_1 n_2}^{(1)} - 2(n_1+n_2 \\
&\quad - 1)\kappa |\Psi_{n_1 n_2}^{(1)}|^2 \Psi_{n_1 n_2}^{(1)}.
\end{aligned} \tag{13}$$

Inserting (12) into (13) and assuming $n_1, n_2 \gg 1$, we have

$$\begin{aligned}
i \frac{\partial}{\partial t} \Psi_{n_{1,2}}^{(1)} &= -\frac{\partial^2}{\partial x^2} \Psi_{n_{1,2}}^{(1)} - 2\kappa n_{1,2} |\Psi_{n_{1,2}}^{(1)}|^2 \Psi_{n_{1,2}}^{(1)} \\
&\quad - 2\kappa \sqrt{n_1 n_2} \left\{ 2 \left| \Psi_{n_{1,2}}^{(1)} \right|^2 \Psi_{n_{2,1}}^{(2)} + \Psi_{n_{1,2}}^{(1)2} \Psi_{n_{2,1}}^{(1)*} \right\}.
\end{aligned} \tag{14}$$

Proceeding, we introduce $\Phi_{n_1, n_2}^{(1)} = \sqrt{\kappa n_{1,2}} \Psi_{n_1, n_2}^{(1)}$ as in the derivation of (10) and normalize t ; we then have from (14)

$$\begin{aligned}
i \frac{\partial}{\partial t} \Phi_{n_{1,2}}^{(1)} &= -\frac{1}{2} \frac{\partial^2}{\partial x^2} \Phi_{n_{1,2}}^{(1)} - |\Phi_{n_{1,2}}^{(1)}|^2 \Phi_{n_{1,2}}^{(1)} \\
&\quad - \left\{ 2 \left| \Phi_{n_{1,2}}^{(1)} \right|^2 \Phi_{n_{2,1}}^{(1)} + \Phi_{n_{1,2}}^{(1)2} \Phi_{n_{2,1}}^{(1)*} \right\}.
\end{aligned} \tag{15}$$

Equation (15) is identical to the corresponding equation in the classical theory.⁸ A perturbation solution can be obtained in the adiabatic approximation. This differs from the approach taken in Ref. 3, which was based on previous work⁷ that did not take soliton interaction into consideration. The last term in curly brackets in (15) explicitly allows for that interaction (interference), which results from the nonlinearity. Furthermore, in the present problem, we can treat it as a perturbation (as in Ref. 8) and write

$$\nu_{m,n}[\Phi_{n,m}^{(1)}] \equiv i(\Phi_m^{(1)*} \Phi_n^{(1)2} + 2\Phi_m^{(1)} |\Phi_n^{(1)}|^2),$$

$$m, n = n_1, n_2, \quad m \neq n.$$

According to the theory described in Ref. 7 and the quantum theory of two-soliton solutions,³ the solitons are initially infinitely far apart. They then interact, although the specifics of their interaction are not spelled out. Finally, they again retreat to infinity, acquiring some phase shift and coordinate displacement as a result of the interaction. In contrast to this approach, here we analyze the interaction itself (see Sec. 5).

The solutions obtained in Ref. 7 then correspond to the asymptotic behavior of the solutions obtained here.

First, we solve Eqs. (15) neglecting soliton interaction (we make no explicit mention of a perturbation in this problem, but both solitons are subject to self-interaction). The result then consists of two isolated solitons undergoing self-interaction:

$$\begin{aligned} \Phi_{n_1, n_2}^{(1)} &= 2\eta_{n_1, 2} \frac{\exp[-2i\zeta_{n_1, 2}(x-x_0)_{1,2} - 2i(\zeta_{n_1, 2}^2 + \eta_{n_1, 2}^2)t]}{\text{ch}[2\eta_{n_1, 2}(x-x_0)_{1,2} + 2\zeta_{n_1, 2}t]} \\ &\equiv 2\eta_{n_1, 2} \frac{\exp[2ip_{n_1, 2}(x-\tau_{n_1, 2}) + i\delta_{n_1, 2}]}{\text{ch}[2\eta_{n_1, 2}(x-\tau_{n_1, 2})]}, \end{aligned} \quad (16)$$

where the $\eta_{n_1, 2}$ are soliton amplitudes, $\zeta_{n_1, 2} \equiv -p_{n_1, 2}$ are soliton momenta, $(x_0)_{1,2}$ are initial soliton coordinates, $\tau_{n_1, 2} = (x_0)_{1,2} + 2p_{n_1, 2}t$, and $\delta_{n_1, 2} = 2(p_{n_1, 2}^2 - \eta_{n_1, 2}^2)t$ are soliton phases. With the normalization (7) for the wave functions $\Psi_{n_1, 2}^{(1)} \equiv \Phi_{n_1, 2}^{(1)} / \sqrt{\kappa n_{1, 2}}$, we obtain the quantization conditions

$$\eta_{n_1, 2} = \frac{\kappa n_{1, 2}}{4}. \quad (17)$$

According to the adiabatic approximation in perturbation theory,⁸ $\eta_{n_1, 2}$, $\tau_{n_1, 2}$, and $p_{n_1, 2}$ in (15) are not constants but functions of t , i.e., $\eta_{n_1, 2} \equiv \eta_{n_1, 2}(t)$, $\tau_{n_1, 2} \equiv \tau_{n_1, 2}(t)$, and $p_{n_1, 2} \equiv p_{n_1, 2}(t)$, and

$$\begin{aligned} \frac{dp_{n_1, 2}}{dt} &= \mp 16\eta_n^3 \exp(-2\eta_n r_n) \cos \psi_n, \\ \frac{d\eta_{n_1, 2}}{dt} &= \mp 16\eta_n^3 \exp(-2\eta_n r_n) \sin \psi_n, \\ \frac{d\tau_{n_1, 2}}{dt} &= 2p_{n_1, 2} + 4\eta_n \exp(-2\eta_n r_n) \sin \psi_n, \\ \frac{d\delta_{n_1, 2}}{dt} &= 2(\eta_{n_1, 2}^2 + p_{n_1, 2}^2) + 8p_n \eta_n \exp(-2\eta_n r_n) \sin \psi_n \\ &\quad + 24\eta_n^2 \exp(-2\eta_n r_n) \cos \psi_n, \end{aligned} \quad (18)$$

where

$$\begin{aligned} r_n &\equiv \tau_{n_1} - \tau_{n_2} > 0, \quad \eta_n \equiv (\eta_{n_1} + \eta_{n_2})/2, \\ p_n &\equiv (p_{n_1} + p_{n_2})/2, \quad \psi_n \equiv 2p_n r_n + \varphi_n \equiv 2p_n r_n + \delta_{n_2} - \delta_{n_1}. \end{aligned}$$

Equations (18) hold when

$$\begin{aligned} |p_{n_1} - p_{n_2}| &\ll p_n, \quad |\eta_{n_1} - \eta_{n_2}| \ll \eta_n, \\ \eta_n r_n &\gg 1, \quad (\eta_{n_1} - \eta_{n_2})r_n \ll 1. \end{aligned} \quad (19)$$

The integrals of the motion in (18) are⁸

$$\begin{aligned} p_n &= \text{const}, \quad \eta_n = \text{const}, \\ Y^2 - 16\eta_n^2 \exp(-2\eta_n r_n) \exp(i\psi_n) &\equiv \Lambda^2 = \text{const}, \\ Y &= \delta p_n + i\delta\eta_n, \end{aligned} \quad (20)$$

where $\delta p_n \equiv p_{n_2} - p_{n_1}$ and $\delta\eta_n \equiv \eta_{n_2} - \eta_{n_1}$.

In physical terms, the first two integrals of the motion simply represent conservation of the total momentum and soliton amplitudes. The last integral of the motion in (20) is more interesting: it amounts to a specific set of parameter combinations for interacting solitons (see Eqs. (27) and (28) in the next section). This is of fundamental importance to the control of quantum chaos (see Sec. 5, where we take soliton interactions in the different channels into consideration from the outset, and also allow for losses). Moreover, while we integrate Eqs. (18), assuming (19) to hold, the integration limits are different from those in Ref. 8. As a result, we have

$$\begin{aligned} \delta p_n(t) &= -\frac{\mu \sinh(4\eta_n \mu t) - \nu \sin[4\eta_n \nu t]}{\text{ch}(4\eta_n \mu t) + \cos(4\eta_n \nu t)} + \delta p_n(0), \\ \delta\eta_n(t) &= -\frac{\nu \sinh(4\eta_n \mu t) + \mu \sin(4\eta_n \nu t)}{\text{ch}(4\eta_n \mu t) + \cos(4\eta_n \nu t)} + \delta\eta_n(0), \end{aligned} \quad (21)$$

$$\begin{aligned} r_n(t) &= r_n(0) + \frac{1}{2\eta_n} \ln \left\{ \frac{1}{2} [\cosh(4\eta_n \mu t) + \cos(4\eta_n \nu t)] \right\} \\ &\quad - 2\delta p_n(0)t, \\ \varphi_n(t) &= \varphi_n(0) - 2\text{arctg}\{\text{th}(2\eta_n \mu t)\text{tg}(2\eta_n \nu t)\} \\ &\quad + 4\eta_n \delta\eta_n(0)t - 2p_n\{r_n(t) - r_n(0)\}, \end{aligned}$$

where the boundary conditions are $\delta p_n(0) \equiv (p_{n_2} - p_{n_1})|_{t=0}$ and $\delta\eta_n(0) \equiv (\eta_{n_2} - \eta_{n_1})|_{t=0}$. In addition,

$$\begin{aligned} \mu &= -\frac{1}{\sqrt{2}} \sqrt{A + \sqrt{A^2 + B^2}}, \quad \nu = \frac{1}{\sqrt{2}} \sqrt{\sqrt{A^2 + B^2} - A}, \\ A &\equiv (\delta p_n^-(0))^2 - (\delta\eta_n(0))^2 - 16\eta_n^2 \\ &\quad \times \exp[-2\eta_n r_n(0)] \cos \psi_n(0), \end{aligned} \quad (22)$$

$$B \equiv 2\delta p_n(0)\delta\eta_n(0) - 16\eta_n^2 \exp[-2\eta_n r_n(0)] \sin \psi_n(0).$$

Making use of the integrals of the motion (20) as well as (21), (22), and (17), we can determine the soliton parameters, and thus the wave functions (16). The two-soliton state vector in the Hartree approximation takes the final form (cf. Ref. 3)

$$\begin{aligned} |\xi\rangle_0 &= \sum_{n_1, n_2} \frac{w_{n_1, n_2}}{\sqrt{n_1! n_2!}} \left\{ \int \Psi_{n_1}^{(1)} a_0^+(x) dx \right\}^{n_1} \\ &\quad \times \left\{ \int \Psi_{n_2}^{(1)} a_0^+(x) dx \right\}^{n_2} |0\rangle, \end{aligned} \quad (23)$$

where the w_{n_1, n_2} are given by (5).

We have thus determined the quantum state of the system for this problem in the present approximation.

It should be noted here that the present lack of coupling between the two channels ($\varepsilon' = 0$) and neglect of soliton interactions in each channel reduces this to an integrable system under the classical approach. At first glance, then, the approximate result (23) ought to be directly comparable with the exact solution. The problems that can arise are well known—in particular, they resemble the problems of secular

terms that can appear in the equation for a nonlinear oscillator.¹⁴ As in the previous case, however, our problem can be examined without regard to the exact solution, and treated as a model (for instance, as a Duffing oscillator; see Sec. 5). More importantly, the quantum case under consideration actually reduces in principle to a multisoliton problem (the number of photons $n_{1,2}$ can take on any value, and the solitons are always coupled by virtue of the nonlinearity and vacuum fluctuations). The problem here, then, is in fact analogous to the classical problem in which coupled multi-soliton aggregates emerge in systems with a nonlocal nonlinearity.¹⁴ The wave function (23), which describes the interference between two quantum soliton states, is just such a realization of a coupled aggregate (see also Sec. 5).

4. NONCLASSICAL EFFECTS INVOLVING COUPLED SOLITONS

In this section, we analyze possible nonclassical effects in coupled states of two solitons. Above all, the discussion will center around photon number fluctuations and nondemolition measurements in such systems.

To start with, consider the instantaneous mean number of photons,

$$\begin{aligned} \langle N \rangle &= \langle \xi | a_0^+(x) a_0(x) | \xi \rangle \\ &\approx \sum_{n_1, n_2} |w_{n_1, n_2}|^2 \{ |\alpha_{10}|^2 |\Psi_{n_1+1}^{(1)}|^2 + |\alpha_{20}|^2 |\Psi_{n_2}^{(1)}|^2 \\ &\quad + 2\text{Re}\{\alpha_{10}^* \alpha_{20} (\Psi_{n_1+1}^{(1)})^* \Psi_{n_2}^{(1)}\} \}, \end{aligned} \quad (24)$$

where α_{10} and α_{20} are complex amplitudes, i.e., $|\alpha_{10,20}|^2$ is the steady-state (initial) number of photons in solitons, and averaging over the states $|\xi\rangle$, which embody characteristics of both solitons [see Eq. (23)], results in the formation of coupled states in this system, as already noted (i.e., it leads to the onset of a pure quantum interference effect between states).

We see from (24), in fact, that quantum solitons are manifested by the superposition of a denumerable set of classical wave packets (solitons). The last term in (24) accounts for the interference of quantum solitons cited above. In the limit

$$n_{1,2} = n_{01,2} \gg 1, \quad \eta_{n_{1,2}}, \eta_n < 1 \quad (25)$$

we obtain from (24) a result that corresponds to the semiclassical approximation:

$$\begin{aligned} \langle N \rangle &\approx |\alpha_{10}|^2 |\Psi_{n_{01}+1}^{(1)}|^2 + |\alpha_{20}|^2 |\Psi_{n_{02}+1}^{(1)}|^2 \\ &\quad + 2\text{Re}\{\alpha_{10}^* \alpha_{20} (\Psi_{n_{01}+1}^{(1)})^* \Psi_{n_{02}+1}^{(1)}\}. \end{aligned} \quad (26)$$

The behavior of the classical wave packets can actually be characterized by the wave functions $\Psi_{n_{1,2}+1}^{(1)}$, and is described by the solutions of (21) (preference being accorded the Hartree approximation). We therefore dwell at some length on the solutions (21) and (22).

If we assume that the amplitudes and velocities for this denumerable set of solitons are all the same at the instant $t=0$, i.e., $\delta\eta_n(t=0)=0$, $\delta p_n(t=0)=0$, we then have for (22)

$$\begin{aligned} \mu &= -4\eta_n \exp[-\eta_n r_n(0)] \sin(\psi_n(0)/2), \\ \nu &= 4\eta_n \exp[-\eta_n r_n(0)] \cos(\psi_n(0)/2). \end{aligned} \quad (27)$$

If we also assume that the classical solitons are still co-phased, i.e., $\psi_n(0)=0$ ($\mu=0$), then

$$r_n(t) = r_n(0) + \frac{4}{\kappa n} \ln \left\{ \frac{1}{2} \left[1 + \cos \left(\frac{2\pi t}{t_s} \exp[-\eta_n r_n(0)] \right) \right] \right\}, \quad (28)$$

$$\varphi_n(t) = -2p_n r_n(t),$$

where $n \equiv n_1 + n_2$ is the total number of photons in solitons, and the new parameter $t_s \approx 8\pi/\kappa^2 n^2$ determines the soliton width (see Ref. 3).

According to (28), we can determine the time required for solitons to merge from the requirement that $r_n(t)=0$, i.e.,

$$t_c = \frac{t_s}{\pi} \exp[\eta_n r_n(0)] \arccos\{\exp[-\eta_n r_n(0)]\}, \quad (29)$$

and likewise, the period of oscillations in the distance between solitons $r_n(t)$, which from (28) we can write in the form

$$T_{\text{osc}} = t_s \exp[\eta_n r_n(0)]. \quad (30)$$

In physical terms, Eq. (30) means that the distance $r_n(t)$ between solitons recurs in times comparable to T_{osc} .

A similar result obtains for $\varphi_n(t)$ and $\delta p_n(t)$, i.e.,

$$\begin{aligned} r_n(t) &= r_n(0) = \text{const}, \quad \varphi_n(t) = -2p_n r_n(0) = \text{const} \\ \delta p_n(t) &= \delta p_n(0) = 0 = \text{const}, \quad \delta \eta_n(t) = \delta \eta_n(0) = 0 = \text{const}. \end{aligned} \quad (31)$$

Note that because the exponential in (30) is large [see (19)], the period of oscillations $T_{\text{osc}} \gg t_s$.

We see, then, that the quantum effects of interest in the present paper are quite prominent in each of the solitons, and only then do they influence soliton interactions (by modifying photon statistics, for example; see below). In particular, when a soliton undergoes strong phase modulation, we have a temporal parameter $t_{ps} < t_s \ll T_{\text{osc}}$ (see Ref. 3). This means, for example, that quadrature squeezing of light, which is produced by just such phase modulation,⁹ first shows up in each of the solitons, and their interactions then give rise to a transfer of fluctuations between them.

On the other hand, it is clear from (30) that if $r_n(0)=0$, $T_{\text{osc}}=t_s$. The solutions (28) then show that the distance between the solitons oscillates with period T_{osc} . In the quantum problem, however, due to the superposition of a denumerable number of such solitons (each with its own amplitude n), they fill the entire $r_n(t)$ plane, and every pair has its own oscillation period $T_{n,\text{osc}}$ for the intersoliton distance. In going to the semiclassical limit, the oscillatory domain shrinks. The upshot [see (26)] is that we wind up with a single pair of solitons, namely the one with the strongest interaction.

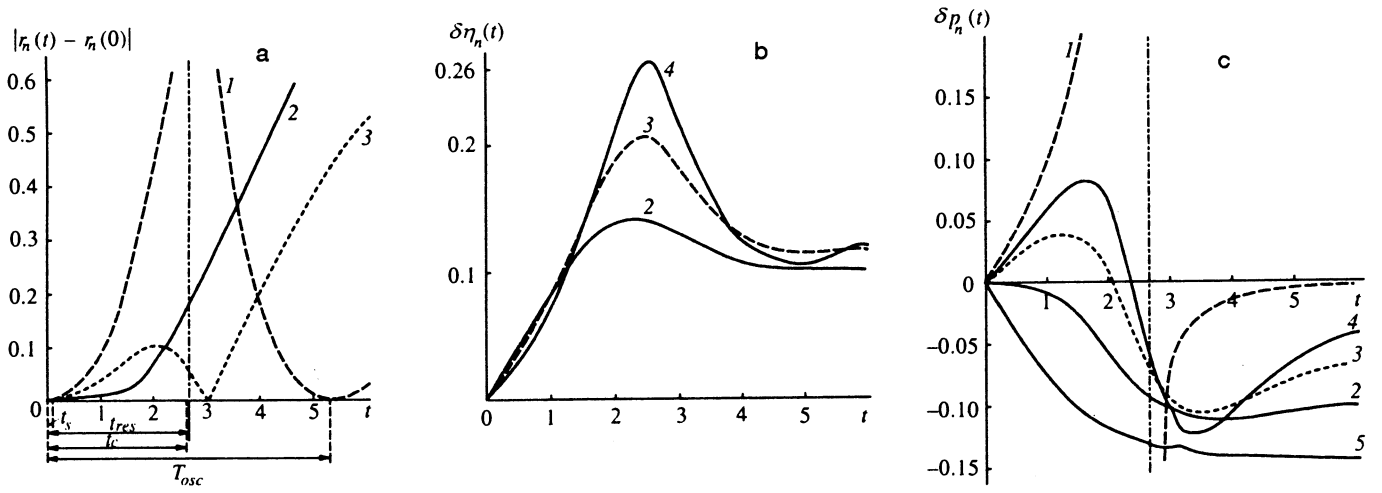


FIG. 1. Calculated behavior of a) position difference $|r_n(t) - r_n(0)|$, b) amplitude difference $\delta\eta_n(t)$, and c) momentum difference $\delta p_n(t)$ as a function of soliton interaction time t (propagation coordinate) (all quantities are normalized). Parameter values are $\delta\eta_n(0)=0$, $\delta p_n(0)=0$, $r_n(0)=2$, $\eta_n(t)=\eta_n(0)=2$. Labeled curves correspond to the following initial differences in phase $\psi_n(0) \equiv 2p_n(0)r_n(0) + \delta_2(0) - \delta_1(0)$: 1) $\psi_n(0)=0$, 2) $\psi_n(0)=\pi/2$, 3) $\psi_n(0)=\pi/3$, 4) $\psi_n(0)=\pi/4$, 5) $\psi_n(0)=\pi$ [the amplitude difference $\delta\eta_n(t)=0$ for $\psi_n(0)=0, \pi$]. Below Fig. 1a we show characteristic scales for soliton interactions with $\psi_n(0)=0$, $t_s \approx 0.098$, $t_{res} \approx 2.68$, $t_c \approx 2.64$, and $T_{osc} \approx 5.35$.

Note that we have not considered dispersive effects in the medium here.³ It can be shown that such group-delay effects show up if $t_{gr} > T_{osc}$, where t_{gr} is the characteristic group delay time. We assume this inequality to hold.

Figures 1a–c show the typical behavior of the coordinate differences $|r_n(t) - r_n(0)|$ (Fig. 1a), amplitude differences $\delta\eta_n(t)$ (Fig. 1b), and momentum differences $\delta p_n(t)$ (Fig. 1c) as a function of time t (in dimensionless propagation coordinates); we have used Eqs. (21) and (27) at fixed η_n (states are labeled with $n \equiv n_1 + n_2 = 8\eta_n/\kappa$). These plots demonstrate that in general [for arbitrary phase difference $\psi_n(0)$] these quantities exhibit complex behavior. More specifically, when $\psi_n(0)=0$ ($4\eta_n\mu t=0$), the system displays a resonance with a characteristic time $t_{res} = \pi/4\eta\nu$ [see (21)], which shows up clearly in Figs. 1a and 1b for the soliton position and momentum differences. In Fig. 1a, we have also indicated the characteristic time scales for interacting solitons: t_s is the period of the solitons, t_{res} is the resonance time, t_c is the time for solitons to coalesce, and T_{osc} is the period of oscillations [see Eqs. (29) and (30)].

Figure 2 shows the behavior of $\delta\eta_n(t)$, $\delta p_n(t)$, and $|r_n(t) - r_n(0)|$ as a function of the initial phase difference $\psi_n(0)/2$, as given by (21) and (27) (with $\delta\eta_n(0) = \delta p_n(0) = 0$). As might be expected, various oscillatory regimes exist under these circumstances (the curves correspond to domains far from the resonance time t_{res}). We also note that when $\psi_n(0)=0$, only the amplitude difference vanishes: $\delta\eta_n(t)=0$ [see (22)].

We now dwell in more detail on the case $\psi_n(0) = \pi + 2\pi k$ ($k=0,1,2,\dots$), i.e., the case in which $\nu=0$. Then from (21) we obtain

$$r_n(t) = r_n(0) + \frac{1}{2\eta_n} \ln \left\{ \frac{1}{2} [1 + \text{ch}(4\eta_n\mu t)] \right\},$$

$$\varphi_n(t) = -2p_n r_n(t) + \pi + 2k\pi, \quad k=0,1,2,\dots \quad (32)$$

It is clear from (32) that the distance between solitons grows logarithmically. For large arguments of the hyperbolic cosine (large t , for instance), and specifically for arguments such that $4\eta_n\mu t \gg 1$, we have from (32) that

$$r_n(t) \approx r_n(0) + 2\mu t, \quad \delta p_n(t) \approx -\mu,$$

$$\delta\eta_n(t) = \delta\eta_n(0) \equiv 0, \quad \varphi_n(t) = -2p_n r(t) + \pi + 2\pi k, \quad (33)$$

i.e., the distance between solitons increases linearly with t . In Fig. 3 we have plotted the calculated distance between solitons $|r_n(t) - r_n(0)|$ as a function of the quantum number (state label) $n \equiv 8\eta_n/\kappa$ at a fixed value of the phase difference, $\psi_n(0) = \pi/3$. The curve shows oscillatory behavior, with an approximately exponential decrease in the amplitude of the oscillations.

For these solitons, with quantum numbers n_1 and n_2 satisfying

$$\text{ch} \left(\frac{\kappa^2 n^2}{4} \exp \left[-\frac{\kappa n}{8} r_n(0) \right] t \sin \frac{\psi_n(0)}{2} \right) + \cos \left(\frac{\kappa^2 n^2}{4} \exp \left[-\frac{\kappa n}{4} r_n(0) \right] t \cos \frac{\psi_n(0)}{2} \right) = 2$$

[see (21), (27)], the distance between them remains constant, i.e., $r_n(t) = r_n(0)$. Note that for large quantum numbers n (for which (33) holds), we also have $r_n(t) \rightarrow r_n(0)$. Indeed, in that case we have

$$\mu \propto n \exp \left[-\frac{\kappa n}{8} r_n(0) \right] \rightarrow 0$$

($r_n(0) \neq 0$), so $|r_n(t) - r_n(0)| \rightarrow 0$ (shown for $\eta_n > 3$ in Fig. 3).

In the general case, for arbitrary $\psi_n(0)$, the behavior of $r_n(t)$ and $\varphi_n(t)$ is not so trivial. We also note here that the perturbation theory solutions have as their limit the solutions

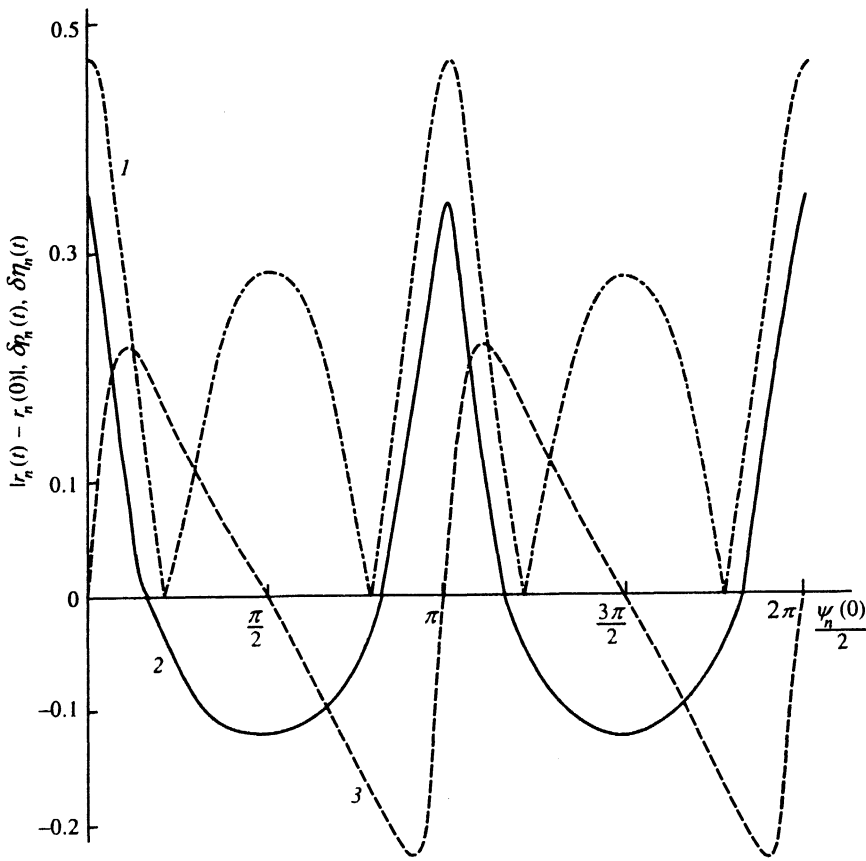


FIG. 2. Calculated dependence of $|r_n(t) - r_n(0)|$ (curve 1), $\delta p_n(t)$ (curve 2), and $\delta \eta_n(t)$ (curve 3) on initial soliton phase difference $\psi_n(0)/2$. Parameter values are the same as in Fig. 1, $t=2$.

of the classical problem,⁸ as well as solutions of the quantum problem,^{1,3} but without the perturbation theory. In the latter case, however, it is not possible for the distance between solitons to oscillate; the nature of that behavior is in fact the subject of our subsequent studies. One of the principal properties of the two-soliton solutions (21) is the dependence of the corresponding quantities on the number of photons. From a physical standpoint, this means that it is possible to obtain qualitatively new quantum properties for coupled solitons, over and above those of isolated solitons.

For the sake of definiteness, consider the generation of squeezed light. This is known to be feasible for a fundamental soliton (a one-soliton solution of the nonlinear Schrödinger equation³). This comes about by virtue of phase modulation in the optical wave packet, and shows up in the

quadrature components⁹ (i.e., we are dealing with quadrature squeezed light). On the other hand, fluctuations in the number of photons remain unchanged, i.e., the photon statistics are unaltered.

If, however, we consider two-soliton solutions, the interaction between the solitons can give rise both to superbunching and antibunching of photons. Physically, this can be attributed to quantum interference between fluctuations (see Ref. 9). Similarly, squeezed states can be shown to exist in other parameters as well, such as soliton positions and momenta.

Consider fluctuations in photon number. We define the operator for the latter (see Ref. 3) to be

$$N = \int_{-\infty}^{\infty} a_0^+(x) a_0(x) dx. \quad (34)$$

Using (23) for $\langle \Delta N^2 \rangle \equiv \langle N^2 \rangle - \langle N \rangle^2$ and the approximations (19), we have for the variance (in the semiclassical limit)

$$\langle \Delta N^2 \rangle \approx \langle N \rangle + |\alpha_0|^4 \{ 2(F_{n_0+2} - F_{n_0+1}) + F_{n_0+2}^2 - F_{n_0+1}^2 \}, \quad (35)$$

$$F_n = \frac{2 \eta_n r_n(t)}{\text{sh}[2 \eta_n r_n(t)]} \cos \psi_n(t).$$

Here we have also set $\alpha_{10} = \alpha_{20} \equiv \alpha_0 / \sqrt{2}$. If in (35) the quantity in curly brackets is negative, i.e., $\langle \Delta N^2 \rangle < \langle N \rangle$, we have antibunching of photons; conversely, for $\langle \Delta N^2 \rangle > \langle N \rangle$, we have superbunching. The statistics are unchanged only when $\langle \Delta N^2 \rangle = \langle N \rangle$.

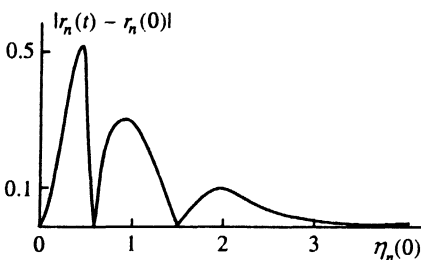


FIG. 3. Calculated dependence of intersoliton distance $|r_n(t) - r_n(0)|$ on total amplitude $\eta_n(0)$ (the quantum number is n , where $\eta_n(t) = \eta_n(0) \kappa(n_1 + n_2)/8 = \kappa n/8$). Other parameters have the same values as in Fig. 1, $\psi_n(0) = \pi/3$, $t=2$.

If in (35) we expand F_n in powers of $2\eta_n r_n(t)$, some straightforward manipulation yields

$$\langle \Delta N^2 \rangle \approx \langle N \rangle - 4|\alpha_0|^4 \sin \psi_{n_0+1} \sin \Delta \psi_{n_0} (1 + \cos \Delta \psi_{n_0} \cos \psi_{n_0+1}), \quad (36)$$

where $\Delta \psi_{n_0} = 0.5(\psi_{n_0+2} - \psi_{n_0+1})$. Assuming $\cos \psi_{n_0+1} \approx 1$, we have from (36) that

$$\langle \Delta N^2 \rangle \approx \langle N \rangle - 8|\alpha_0|^4 \psi_{n_0+1} \sin \Delta \psi_{n_0} \cos^2(\Delta \psi_{n_0}/2). \quad (37)$$

Thus, photons will antibunch if we simultaneously have either $\psi_{n_0+1} > 0$, $\sin \Delta \psi_{n_0} > 0$ or $\psi_{n_0+1} < 0$, $\sin \Delta \psi_{n_0} < 0$. On the other hand, when $\delta \eta_n(0) = 0$, $\delta p_n(0) = 0$, and $\psi_{n_0+1}(0) = \psi_{n_0+2} = 0$, we have from (28), (30), and (31) that $\langle \Delta N^2 \rangle \sim \langle N \rangle$ on timescales T_{osc} , i.e., the photons still have Poisson statistics. The latter property of interacting solitons can be used for quantum nondemolition measurements (see Appendix 2).

5. QUANTUM SOLITONS IN TUNNEL-COUPLED FIBERS. CONTROL OF QUANTUM CHAOS

In this section we will be interested in the propagation of quantum solitons, first in the presence of self-interaction in each channel, and then in the presence of cross-interactions between two channels. We will examine this problem in a special type of optical fiber with efficient intermode energy exchange (double-stranded tunnel-coupled fiber optic waveguide¹³). This problem is certainly of experimental interest, and the information presented in this section is fundamental to the present paper.

As we have shown above, coupled solitons do indeed possess extremely interesting quantum properties, such as sub-Poissonian photon statistics. Furthermore, it turns out to be possible to conduct quantum nondemolition measurements of the number of photons in one soliton (the signal) via the other (the probe), or of the difference in photon numbers (see Appendix 2).

On the other hand, in a classical analysis of the propagation of coupled soliton-like entities in a system described by a class of nonintegrable equations,⁵ one may encounter nontrivial (chaotic) interaction dynamics. The construction of a quantum theory of interaction for such objects therefore makes it possible to address the issue of quantum chaos in general, and the control of quantum chaos in particular (see Ref. 6, for example).

Our discussion begins with the construction of wave functions for interacting solitons in a tunnel-coupled fiber optic waveguide (see also Appendix 1). The statement of this problem was presented in Sec. 2 [see Eq. (11)]. Here, however, we also take fiber losses (attenuation) into account. For simplicity, we stay with a commonly adopted phenomenological description, without dwelling on the formalities of the Hamiltonian approach.

To begin with, we rewrite (11) in the form

$$i \frac{\partial}{\partial t} \Phi_n^{(1)} = -\frac{1}{2} \frac{\partial^2}{\partial x^2} \Phi_n^{(1)} - |\Phi_n^{(1)}|^2 \Phi_n^{(1)} + \varepsilon' \Phi_k^{(2)} - i\gamma \Phi_n^{(1)}, \quad (38)$$

$$i \frac{\partial}{\partial t} \Phi_k^{(2)} = -\frac{1}{2} \frac{\partial^2}{\partial x^2} \Phi_k^{(2)} - |\Phi_k^{(2)}|^2 \Phi_k^{(2)} + \varepsilon' \Phi_n^{(1)} - i\gamma \Phi_k^{(2)}.$$

The last terms on the right-hand sides in Eqs. (38) are responsible for fiber losses (the attenuation factor is γ). Formally, these equations describe the "relaxation" of the wave functions (a proper systematic treatment of losses in the Schrödinger formalism is a problem of interest in its own right, and will not be considered here).

This interpretation, however, is tenable when γ is small, which then enables one to work in the adiabatic approximation and perturbation theory. Moreover, a description of the problem in the Hartree approximation, which we have adopted, is closer to the classical approach, so the wave functions $\Phi_{n,k}^{(1,2)}$ can be considered classical wave packets (solitons). This ensures consistency of the quantum theoretical results with the solution of the classical problem. We also note that the introduction of noise sources in the classical description can fundamentally affect the behavior of a nonlinear system.¹⁴

The procedure for solving (38) is similar to the one employed above. We can therefore immediately write out the soliton solutions [cf. (16)]:

$$\Phi_{n,k}^{(1,2)} = 2\eta_{n,k} \frac{\exp[2ip_{n,k}(x - \tau_{n,k}) + i\delta_{n,k}]}{\text{ch}[2\eta_{n,k}(x - \tau_{n,k})]}, \quad (39)$$

where $\eta_n \approx \kappa n/4$ and $\eta_k \approx \kappa m/4$ (we assume that $m \approx n \gg 1$ and for convenience we will re-indicate the symbols $n \equiv n_1, k \equiv n_2$) are the soliton amplitudes, the $\delta_{n,k}$ are their phases, and the $p_{n,k}$ are their momenta [see (16)]. As before, we assume that all of these quantities depend on t .⁵

In the present case, the perturbing term in the nonlinear Schrödinger equations (38) takes the following form [we make the same assumptions about the soliton interactions in each channel as before—see the explanations accompanying (15) and (16)]:

$$v_{i,j}[\Phi_{ij}] = -\gamma \Phi_i^{(1,2)} - i\varepsilon' \Phi_j^{(2,1)}, \quad i, j = n, k, \quad i \neq j.$$

We then ultimately obtain for the soliton parameters under consideration the equations (cf. Ref. 5)

$$\dot{p}_{n_{1,2}} = \pm 2\eta_n \varepsilon' \frac{r_n \text{ch } r_n - \text{sh } r_n}{\text{sh}^2 r_n} \cos \psi_n,$$

$$\dot{\tau}_{n_{1,2}} = 2p_{n_{1,2}} + \frac{\varepsilon'}{2\eta_n} \frac{r_n^2}{\text{sh } r_n} \sin \psi_n, \quad (40)$$

$$\dot{\eta}_{n_{1,2}} = \pm 2\eta_n \varepsilon' \frac{r_n}{\text{sh } r_n} \sin \psi_n - 2\gamma \eta_{n_{1,2}},$$

$$\dot{\delta}_{n_{1,2}} = 2p_{n_{1,2}} \dot{\tau}_{n_{1,2}} + 2(\eta_{n_{1,2}}^2 - p_{n_{1,2}}^2) + \frac{\varepsilon' r_n}{\text{sh } r_n} \left(\frac{r_n}{\text{th } r_n} - 2 \right) \cos \psi_n,$$

where $\dot{p}_{n_{1,2}} \equiv dp_{n_{1,2}}/dt$, $\dot{\eta}_{n_{1,2}} \equiv d\eta_{n_{1,2}}/dt$, $\dot{\tau}_{n_{1,2}} \equiv d\tau_{n_{1,2}}/dt$, $\dot{\delta}_{n_{1,2}} \equiv d\delta_{n_{1,2}}/dt$, and we denote the distance between solitons by $r_n = 2\eta_n(\tau_{n_1} - \tau_{n_2})$. In addition, $\eta_n = \frac{1}{2}(\eta_{n_1} - \eta_{n_2})$,

$p_n = \frac{1}{2}(p_{n_1} - p_{n_2})$, and $\psi_n = 2p(\tau_{n_1} - \tau_{n_2}) + \delta_{n_2} - \delta_{n_1}$. We have derived Eqs. (40) under the same approximation as (18). The following remark is useful in connection with the latter statement.

For the nonlinear Schrödinger equation that we consider here, it is of fundamental importance that there exist perturbations that lead to the establishment of coupling between the solitons, regardless of whether it arises as a result of energy exchange between the two strands ($\varepsilon' \neq 0$) or direct interaction (apart from self-interaction effects) between two solitons in each of the fibers. The actual form of the perturbing term, be it $\nu_{n,m}[\Phi_{n,m}^{(1)}]$ in Eq. (15) or $\nu_{i,j}[\Phi_{n,k}^{(1,2)}]$ in Eq. (38), is therefore probably not so important in a physical sense, and the results that we have obtained in the present section are in fact applicable to the case considered in Sec. 3, with coupling between the solitons. Naturally, the specific form of the resulting wave functions depends on the type of interaction considered (mathematically, these are different problems), and here it would be of some interest to clarify the analogies between the interacting solitons in these two situations.

Straightforward manipulation of Eqs. (40) reduces them to equations for ψ_n , r_n , $\delta p_n \equiv p_{n_2} - p_{n_1}$, and $\delta \eta_n \equiv \eta_{n_2} - \eta_{n_1}$:

$$\begin{aligned} \ddot{r}_n + 2\gamma \dot{r}_n &= 16\eta_n^2 \varepsilon' \frac{r_n \operatorname{ch} r_n - \operatorname{sh} r_n}{\operatorname{sh}^2 r_n} \cos \psi_n = 0, \\ \ddot{\psi}_n + 2\gamma \dot{\psi}_n + 16\eta_n^2 \varepsilon' \frac{r_n}{\operatorname{sh} r_n} \sin \psi_n &= 0, \\ \delta \dot{\eta}_n + 4\eta_n \varepsilon' \frac{r_n}{\operatorname{sh} r_n} \sin \psi_n &= 0, \\ \delta \dot{p}_n + 4\eta_n \varepsilon' \frac{r_n \operatorname{ch} r_n - \operatorname{sh} r_n}{\operatorname{sh}^2(r_n)} \cos \psi_n &= 0. \end{aligned} \quad (41a)$$

Here the solutions for p_n and η_n take the form

$$(p_{n_1} + p_{n_2})/2 \equiv p_n = \text{const}, \quad \eta_n = \eta_n^{(s)} e^{-2\gamma t}, \quad (41b)$$

where the $\eta_n^{(s)}$ are the total soliton amplitudes at $t=0$. Continuing, we expand the last terms in Eqs. (41a) in powers of r , which yields

$$\begin{aligned} \ddot{r}_n + 2\gamma \dot{r}_n - \frac{16}{3} \eta_n^2 \varepsilon' r_n \cos \psi_n &= 0, \\ \ddot{\psi}_n + 2\gamma \dot{\psi}_n + 16\eta_n^2 \varepsilon' \sin \psi_n &= 0, \\ \delta \dot{\eta}_n + 4\eta_n \varepsilon' \sin \psi_n &= 0, \\ \delta \dot{p}_n + \frac{4}{3} \eta_n \varepsilon' r_n \cos \psi_n &= 0. \end{aligned} \quad (42)$$

In conjunction with (41b), Eqs. (42) determine the soliton parameters, and thus the wave functions (39).

It is fundamentally important in Eqs. (42) that the amplitude η_n depends on the state label n [see (39)]; this is true of the other quantities as well. In other words, as we noted above, an optical wave packet in the quantum problem is a weighted sum of a denumerable set of classical solitons (with

differing n) [see (24) and Ref. 9]. This is actually the decisive factor that enables one to consider the problem as stated.

Indeed, we have reduced the solution of the quantum problem, in the context of our approach, to a set of equations that can be analyzed with no particular difficulty. Specifically, the quantities that appear in Eq. (42) can be investigated via a phase-space approach, since we are dealing here with individual "classical" solitons, each with its own value of n . The overall behavior of the quantum system will then in fact be determined by a superposition of such objects, whose phase portraits (trajectories) can be calculated using standard methods.⁵ This approach admits of an analogy with a solution technique based on path integrals.^{4,15}

We now consider various limiting cases.

5.1. Harmonic oscillation regime

We assume the linear coupling parameter between two strands of a tunnel-coupled fiber waveguide to be constant in time ($\varepsilon' = \text{const}$). Equations (42) can then be solved in the following manner. To start with, we set $\gamma=0$ for simplicity [in which case $\eta_n \equiv \eta_n^{(s)}$ is an integral of the motion; see (41b)], and for convenience we put

$$\Omega_n^2 = 16\eta_n^2 \varepsilon'. \quad (43)$$

With these assumptions, Eqs. (42) yield

$$\begin{aligned} \ddot{r}_n - \frac{1}{3} \Omega_n^2 r_n \cos \psi_n = 0, \quad \ddot{\psi}_n + \Omega_n^2 \sin \psi_n &= 0, \\ \delta \dot{\eta}_n + \frac{1}{4\eta_n} \Omega_n^2 \sin \psi_n = 0, \quad \delta \dot{p}_n + \frac{1}{12\eta_n} \Omega_n^2 r_n \cos \psi_n &= 0. \end{aligned} \quad (44)$$

Equations (44) for r_n and ψ_n are well known—they are of the same form as the equations for coupled nonlinear oscillators (with different n) that have the same mass and natural frequencies Ω_n (see Ref. 14). We can formally write the Hamiltonian as

$$H_n = \frac{1}{2} \dot{\psi}_n^2 - \Omega_n^2 \cos \psi_n, \quad (45)$$

where $\dot{\psi}_n$ plays the role of the momentum and ψ_n , the position. In the present (optical) problem, the ψ_n are the phases of the classical solitons, and the $\delta \omega_n \equiv \dot{\psi}_n \equiv d\psi_n/dt$ are the frequency deviations (chirp). For some fixed value of n , the phase portrait is trivial, and has been treated in the literature numerous times (see Ref. 14, for example). Equilibrium states correspond to the points

$$\begin{aligned} \delta \omega_n^{(s)} = 0, \quad \sin \psi_n^{(s)} = 0, \\ \psi_n^{(s)} = \pi k, \quad k = 0, \pm 1, \dots \end{aligned} \quad (46)$$

The behavior of the system near these equilibrium points is of the greatest interest.

As we showed above [see (31), (32) and Eqs. (B11)–(B14) in Appendix 2], in those regions, coupled-soliton amplitude (or phase) fluctuations are stabilized, and quantum nondemolition measurements of signal soliton photon numbers are possible. Thus, for the $\psi_n^{(s)}$ in (46), we can use (44) to obtain

$$\delta \eta_n(t) = \delta \eta_n(t=0) = \text{const}, \quad (47)$$

i.e., the soliton amplitudes are integrals of the motion. It is important to note here, however, that satisfying (46) is not a sufficient condition from the standpoint of the general theory of quantum nondemolition measurements [including, in the present instance, high-precision (reproducible) position measurements on the signal soliton]. It is also necessary that there be interactions between the (signal and probe) solitons that are periodic in time. In the present case, we are dealing with oscillations in the distance r_n between solitons [see (30)]. The equation for r_n in (44) corresponds to harmonic oscillations only when $\Omega_n^2 \cos \psi_n < 0$. In (46), we must therefore eliminate values of $\psi_n^{(s)}$ with even k , whereupon (44) yields

$$\ddot{r}_n + \frac{1}{3}\Omega_n^2 r_n = 0, \quad \psi_n^{(s)} = 2\pi k + \pi, \quad k=0,1,2,\dots$$

According to (48), then, quantum nondemolition measurements of the position of the signal soliton are feasible at time intervals

$$T_{n,\text{osc}} = 2\pi\sqrt{3}/\Omega_n, \quad (49)$$

and for the momentum difference δp_n between the solitons, we obtain from (44) $\delta p_n \equiv \delta p_n(0) = \text{const}$.

Thus, in the present case, quantum nondemolition measurements can be made

a) at equilibrium points for phase differences between two coupled solitons, i.e., where $\psi_n^{(s)} = 2\pi k + \pi$, $k=0,1,2,\dots$;

b) when the distance between solitons oscillates; the period of these oscillations is $T_{n,\text{osc}} = 2\pi\sqrt{3}/\Omega_n$.

These two conditions yield the integrals of the motion $\delta p_n \equiv \delta p_n(0) = \text{const}$ and $\delta \eta_n(t) \equiv \delta \eta_n(0) = 0 = \text{const}$. Note that the required phases $\psi_n^{(s)}$ in the present case are shifted by π relative to the phase difference ψ_n for two-soliton solutions [see (31)].

5.2. Parametric oscillations

Consider the time-variable quantity $\varepsilon' \equiv \varepsilon'(t)$, which characterizes the linear coupling between solitons in two fiber strands, and which plays the role of the longitudinal position (along the fiber).¹² We assume the time dependence to be harmonic, $\varepsilon' = \varepsilon_0 + \beta \cos(\chi t)$, where ε_0 is the regular part of ε' , β is the modulation amplitude, and χ is a periodicity parameter (analogous to the reciprocal lattice vector in the spatial Bragg diffraction problem⁹). The oscillator frequencies Ω_n [see (44)] will then be time-dependent:

$$\begin{aligned} \Omega_n^2 &\equiv \Omega_n^2(t) = 16\eta_n^2[\varepsilon_0 + \beta \cos(\chi t)] \\ &= \Omega_{n,st}^2[1 + \varepsilon_1 \cos(\chi t)], \end{aligned} \quad (50)$$

where $\Omega_{n,st}^2 \equiv 16\eta_n^2\varepsilon_0$ and $\varepsilon_1 \equiv \beta/\varepsilon_0 \ll 1$.

We begin our analysis of Eqs. (44) in this case with the equation for ψ_n , in which we are dealing with nonlinear parametrically excited oscillators (for each n).

The Hamiltonian, as was true for (45), can be cast in the form

$$H'_n = H_n + \varepsilon_1 V_n \cos(\chi t), \quad (51)$$

where H_n is the Hamiltonian of the corresponding unperturbed system (45) (with the replacement $\Omega_n^2 \rightarrow \Omega_{n,st}^2$), $\varepsilon_1 V_n$ is the perturbed part (ε_1 is the small perturbation parameter for this problem), and $V_n = -\Omega_n^2 \cos \psi_n$.

It is well known¹⁴ that such a system will have domains of instability, and that stochastic processes can develop. The web-like boundaries of the stochastic regions are concentrated near the separatrices (equilibrium states), and are specified by^{5,14}

$$|H_n - H_n^{(s)}| \leq \Omega_{n,st}^2 \varepsilon_1 \left(\frac{\chi}{\Omega_{n,st}} \right)^3 \exp\left(-\frac{\pi\chi}{2\Omega_{n,st}} \right), \quad (52)$$

where H_s is the value of the Hamiltonian at the separatrix. The stochastic region thus decreases exponentially, and its maximum width (the stochastic layer) is of order ε_1 .

Under certain conditions (selected values of the parameters), such a system can make the transition to dynamical chaos, which can come about through overlapping resonances. Here we are dealing with the appearance of a stochastic web with islands of stable motion.¹⁴ If, making use of (50), we allow for a dissipative term [see (41a)] in Eqs. (44) for ψ_n , the system will have an attractor. The process will then entail the destruction (or alteration) of the problem's integrals of the motion.

This sort of picture for the onset of chaotic behavior (via the phase difference between the two solitons, in the present case) applies to the classical description. The passage to the quantum limit follows the procedure outlined above.

We have then a set of classical parametric oscillators with frequencies Ω_n . In the general case, however, when one sums over states of all oscillators, from the standpoint of the classical criteria for stochastic behavior (52) it is difficult to say much about the quantum-mechanical problem.

In fact, even the criterion (52) for the advent of a stochastic layer will obviously not be satisfied for all n , so that certain of the solitons that enter into the sum will be perfectly regular. On the other hand, each of the oscillators to which (52) applies will have its own stochastic web, and the result of superposing them all will be quite complex. Control of such a quantum system will be discussed in the next subsection; we now turn to an analysis of the rest of Eqs. (44), with (50) taken into account.

We know, to begin with, that r_n satisfies the Mathieu equation:

$$\ddot{r}_n + \frac{1}{3}\Omega_{n,st}^2[1 - |\varepsilon_1| \cos(\chi t)]r = 0. \quad (53)$$

Here we again assume that the stabilization requirement leading to the possibility of quantum nondemolition measurements, $\cos \psi_n = -1$, holds for the phase difference between the two modes. We also assume that the small parameter $\varepsilon_1 < 0$.

The solutions of Eq. (53) have domains of instability, which in the present problem come into consideration for certain intersoliton distances. The boundaries of the first such domain (parametric resonance) are determined (see Ref. 14, for example) by

$$-\sqrt{\frac{\Omega_{n,st}^2}{12} - 4\gamma^2} < \delta < \sqrt{\frac{\Omega_{n,st}^2}{12} - 4\gamma^2},$$

where δ is a small frequency offset between $\Omega_{n,st}/\sqrt{3}$ and χ (γ is the damping factor). The value of r_n increases in the unstable domains, so that as mentioned above, quantum non-demolition measurements of the signal soliton position require that we be outside those domains. Equation (53), on the other hand, has no stochastic eigensolutions.

In the general case, then, this type of solution depends solely on the behavior of the phase difference ψ_n [see (42), (44)], which then determines the dynamical motion for all other quantities in (44).

When a nonlinear term and damping are present, Eqs. (53) in and of themselves can result in chaotic behavior (via period-doubling bifurcations).¹⁴ This corresponds to a consideration of higher-order soliton-like solutions in tunnel-coupled fiber waveguides (see Secs. 2 and 3, and Appendices 1 and 2), in which the nonlinearity shows up as a perturbation. Instead of Eqs. (42) for r_n and ψ_n , we then have

$$\begin{aligned} \ddot{r}_n + 2\gamma\dot{r}_n - \frac{2}{3}\kappa_n(3\kappa_n + \varepsilon')r \cos \psi_n + \kappa_n^2 r_n^2 \\ \times \cos \psi_n + 2\kappa_n^2 \cos \psi_n = 0, \quad \ddot{\psi}_n + 2\gamma\dot{\psi}_n + 2\kappa_n(\kappa_n - \varepsilon') \\ \times \sin \psi_n + \kappa_n^2 r_n(r_n - 2)\sin \psi_n = 0, \end{aligned}$$

where $\kappa_n = 8\eta_n^2$. We thereby obtain a pair of coupled equations that can be analyzed using standard numerical methods.¹⁴

5.3. Discussion. Control of a quantum chaotic state

Let us briefly summarize. The physical model employed to analyze the given problem in this paper is in fact based on the semiclassical approximation, in which the number of photons in the solitons is large. This is why one can easily allow for damping in the original equations (38).

On the other hand, even in the semiclassical approximation, macroscopic states of light can exhibit quantum properties. Above all, this applies to the uncertainty relationship governing the variance of conjugate quantities. Squeezed light, with nonclassical photon statistics, provides an example of this phenomenon.¹⁶ In the Hartree approximation, which we use here, the interacting solitons are a superposition of a denumerable set of classical solitons (cf. Refs. 3, 9) whose behavior gives rise to complicated system dynamics. In interpreting the results, it may be useful to employ the quantum chaos criteria for the system wave functions or energy spectrum.⁶ Another possibility, which we dealt with above, is to search for stochastic behavior in the classical analog of the quantum system under study. We can then bring to bear the powerful and well-developed methods used to study chaos in classical systems.¹⁴ The behavior of quantum solitons can be quite complex, however, as both the superposition of classical solitons and their interference must be taken into account, leading to significant departures from the classical analog of the problem.

At first glance, with this complicated an array of phenomena, the prospects for controlling quantum chaos would appear to be bleak. However, we do have at our disposal methods of influencing both the noise level in a quantum system (squeezed light) and the role played by the measure-

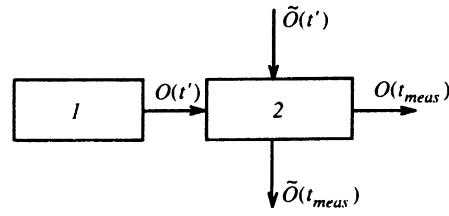


FIG. 4. Block diagram demonstrating the feasibility of quantum nondemolition measurements of the chaotic quantity $O(t')$. 1) Quantum chaotic system generating the quantity $O(t)$; 2) device implementing quantum nondemolition measurements of $O(t')$. Here $\tilde{O}(t')$ is the probe quantity employed to make the quantum nondemolition measurements.

ment process (specifically, quantum nondemolition measurements), which enable us to contemplate some approaches to this problem.

Indeed, the foregoing analysis leads us to believe that system fluctuations grow in regions of unstable motion. More precisely, the lower bound in the uncertainty relations on the product of fluctuations of conjugate (quadrature) quantities rises, an observation upon which a number of workers have focused attention (see a discussion of the quantum Hénon–Heiles model in Ref. 6, for example). This of course does not rule out the possibility of generating squeezed light in such a system for just one quadrature component. But because the overall product of the variances of the two quadrature components increases, what we actually have is an increase in the total system noise.

On the other hand, when one makes quantum nondemolition measurements in some system (see Appendix 2), noise is suppressed. Notably, the lower bound on the uncertainty relation (for example, between the number of particles and the phase of the light field) is unchanged as a result of such measurements—it remains at a minimum.¹⁷ In our opinion, this is precisely the key issue in the control of quantum chaos. There would seem to be two possible paths to such control.

The first is to produce a complicated description of the interaction between the quantum objects (solitons) in the system, and to control the latter within the confines of that system (as discussed above). Subsequent interactions of such objects (detection, for instance), can then be treated classically.

The second is to either initially or subsequently influence the complex system thus produced (see Fig. 4). In the process, those influences are quantum effects.

On the other hand, this problem is closely related to observation of the eigenvalues (measurement) of a chaotic quantity, as well as to the emergence of the system from such a chaotic state in the quantum problem. To clarify the point, we now dwell on this problem in more detail, and analyze the quantum nondemolition measurement technique itself.

Let $O(t)$ be an observable (measurable) physical quantity. The essence of the quantum nondemolition measurement is that by measuring $O(t)$ at some instant of time t , we obtain complete information about its prior history, i.e., its behavior at times $t < t_{meas}$ (cf. Ref. 18). It is also possible to

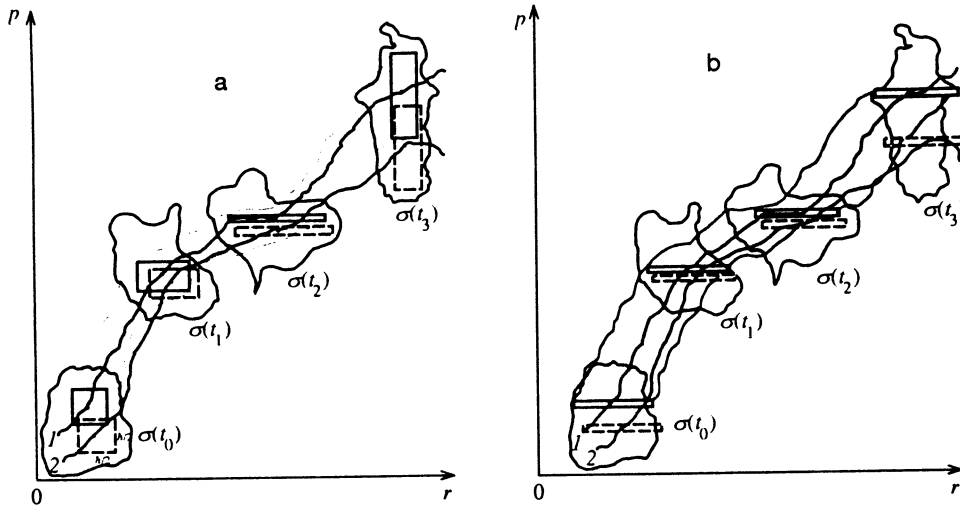


FIG. 5. Evolution of the phase volume $\sigma(t)$ in the (r, p) phase plane (p is the momentum, r the position). Here $\sigma(t_0)$ represents the feasible initial conditions. For clarity, we show only two phase trajectories, labeled 1 and 2. In the quantum problem, each one is uncertain (in the classical sense); for clarity, the “uncertainty envelope” is shown only for trajectory 1. Rectangles (cells) within that envelope (shown dashed for trajectory 2) indicate the measurement errors in p . For squeezed states, it is not always the case that $\langle \Delta p^2 \rangle < \hbar/2$ (a), while for quantum nondemolition measurements (b), the uncertainty envelope surrounds the trajectory out to a finite width that depends on the degree to which the measurement is not ideal (measurement error $\langle \Delta p^2 \rangle \ll \hbar/2$).

take sampled measurements at well-defined times t_{meas} .

In other words, by making such high-precision measurements, we can reduce the quantum uncertainty in measurements of $O(t)$. This occurs, of course, at the expense of increased uncertainty in the quantity conjugate to $O(t)$.

The basic point here, however, is that in general, such quantum measurements cannot yield information about regularity or the lack of it (chaos) in the behavior of $O(t)$.

In fact, as shown in Ref. 19, it is precisely under the conditions of sampled quantum nondemolition measurements of the position of a quantum object that one can detect chaotic behavior, while no such measurements can be made in a regular domain. This property of a quantum system can be used to observe quantum chaos. It corresponds to the first of the two possibilities mentioned above for implementing quantum nondemolition measurements of chaotic systems.

In the present problem, however, it is exactly in the domain of regular behavior of the system that we have analyzed the possibility of making quantum nondemolition measurements of the difference in photon numbers, momenta, or soliton positions.

Requiring consistency between these two cases brings us to the fact that quantum nondemolition measurements disrupt the chaotic regime. Nevertheless, in no way does this mean that such chaotic behavior cannot show up in the present problem.

Figure 4 is a block diagram of the proposed measurement scheme, in which a stochastic (irregular) quantity $O(t')$ is measured nonperturbatively in a quantum measurement setup with the aid of the quantity $\tilde{O}(t)$. Interestingly enough, in a quantum nondemolition measurement, the interaction between $O(t)$ and $\tilde{O}(t)$ is regular. This then comprises the aforementioned second possibility in the quantum chaos control problem.

Actually, by measuring a quantity at some time t_{meas} , we can deduce something about its chaotic behavior at earlier times t , with $t' \approx t \leq t_{\text{meas}}$. We thus see that quantum nondemolition measurements can be a genuine instrument for controlling the state of a quantum chaotic system. We also note that this does not rule out the possibility of simulta-

neously making another kind of quantum nondemolition measurement—a high-precision measurement of the number of photons in the signal soliton, or its momentum (see Appendix 2).

We now describe the measurement method using squeezed light, with which one can also suppress quantum fluctuations and improve the observational accuracy of $O(t)$. In the present problem, we make use of squeezed states for the difference in soliton photon numbers (see Sec. 4) or the difference in their positions, as described by the Mathieu equation (53). Indeed, it is well known in the latter case that in a region where the corresponding quantity is increasing [here we mean $r_n(t)$], i.e., in a domain of instability of (54), squeezed states of a parametrically excited oscillator are produced that have an exponentially growing squeezing coefficient.²⁰

We believe, however, that the main problem concerns the relationship among the characteristic time scales that govern the production of squeezed states (the evolution of quantum fluctuations), and the times for instability (chaos) to develop in such a system. In large measure, this has to do with dissipative (non-Hamiltonian) chaotic systems, in which the extent of squeezing is limited by dissipation. In order for the behavior of such systems to be observable, the aforementioned time scales must bear a certain relationship to one another, and this is not always the case (cf. Refs. 21, 22, and 25).

By way of illustration, consider the phase-space diagrams in Figs. 5a and 5b. We have plotted portions of phase trajectories within a phase volume σ in the position-momentum plane of a quantum particle (at certain times in the interval $t_0 < t < t_3$). According to the uncertainty principle, every trajectory will always have some “uncertainty envelope,” which will generally vary with time. In Fig. 5a, for example, we see that when we observe the particle momentum at successive times t_0, t_1, t_2, t_3 , the uncertainty in the momentum is different for each.

Thus, for example, at $t = t_0$, the uncertainty corresponds to a cell in the phase plane with dimensions of order $\hbar/2$ (a coherent state). We have a squeezed state (for momentum

fluctuations) at times $t=t_1$ and $t=t_2$, and it turns out to be possible to track such a trajectory with higher accuracy, which depends on the degree of squeezing. Subsequently, we see that at $t=t_3$ the “uncertainty cell” has grown (it exhibits larger momentum fluctuations). Accurate measurements can thus only be made at $t=t_1$ and $t=t_2$. For this to be so, however, the mere existence of a squeezed state is not at all sufficient, and the two cases given, involving the complex, convoluted behavior of a stochastic system, can differ significantly when we consider a bundle of possible trajectories in some phase volume²² and two nearby trajectories do not differ in terms of their uncertainties (Fig. 5a, $t=t_1$).

The situation is different when we carry out quantum nondemolition measurements (Fig. 5b). The uncertainty envelope is then related to the measurement accuracy, which remains high and constant for all trajectories in the course of continuous (at all instants of time) measurements.

In the first case, of course, by controlling the degree of squeezing of fluctuations and the uncertainty-cell orientation, we can measure some property of a chaotic system at a given time to the required accuracy. We might, for example, illuminate such a system with specially prepared light in a squeezed state, and thereby have an additional (external) parameter with which to control the measurement process.²³

Obviously, however, such states themselves may be considered a source of additional perturbations conveyed to the system from outside, which can randomly disrupt the evolution of the system. As a consequence, we again end up with the need to make quantum nondemolition measurements. Special procedures for making such measurements are discussed in Ref. 24.

Quantum nondemolition measurements thus provide a universal method of controlling a quantum chaotic system. From a formal mathematical standpoint, this derives from the fact that the analysis underlying quantum nondemolition measurements goes beyond the scope of perturbation theory, and holds for long time intervals, over which system evolution can be examined. In contrast, squeezed light is usually linked to certain constraints in the theory on the length (time) scale of the interaction, the number of photons, and so on.⁹

6. CONCLUSION

In this paper we have analyzed, for optically coupled soliton-like entities, such fundamental problem as the onset and structure of chaos, and the feasibility of controlling it. We have discussed these states in various parameters (including the number of photons) of two interacting wave packets.

One important feature of the overall nonlinear dynamical system considered here is the presence of linear energy exchange between the interacting modes, which in fact constitutes distributed feedback and plays the role of an energy support for the inherently nonlinear interaction of the two modes. The latter ensures the necessary phase relations between the coupled modes (excitation of conjugate fields), which leads to a redistribution and attenuation (amplification) of the noise in certain components of the light in such a system.

A nontrivial aspect of our work here is that the given states can be determined in a quantum system. Indeed, the

problem of quantum chaos has thus far been extremely narrowly defined and not fully solved, entailing the analysis of chaotic phenomena in dynamical systems and in their quantum properties.⁶ In the present case, however, the production of squeezed light and the implementation of a nondemolition measurement technique for a given quantum system (coupled solitons) has made it possible to investigate problems in the semiclassical approximation.

The basis for doing so has been our previous result⁹ for the propagation of pulsed laser beams in a nonlinear distributed feedback system. Specifically, we have shown for this case that a quantum wave packet in the Schrödinger picture is a superposition of a denumerable set of differently shaped classical pulses (beams) with different instantaneous phases, and that the pulses are summed with different weights. Such an approach makes it easy to examine the correspondence between the quantum and classical description, making it possible to obtain specific results.

In essence, we have been discussing the feasibility of representing and interpreting a wave function in terms of a conventional classical field.²⁶ This field interpretation, it turns out, is actually feasible and is likely to be especially useful in treating the propagation of chirped laser pulses in a nonlinear medium, which corresponds to the problem we have considered here.

We thank the referee for constructive criticism and valuable remarks, which we incorporated in the final version of this paper. This work was partially supported by the Russian Fund for Fundamental Research and the International Science Foundation (Grant No. NYW000).

APPENDIX 1

The nonlinear Schrödinger equation and its soliton solutions

We briefly discuss the class of equations considered in the present paper, which give rise to soliton-like solutions. We have in mind here the nonlinear Schrödinger equation, which we write in the form

$$i\tilde{q}_t + \tilde{q}_{\xi\xi} + 2|\tilde{q}|\tilde{q}^2 = 0. \quad (A1)$$

Another model for the formation of solitons in the context of this class of equations is one of the same type as in Eq. (A1), but with the independent variables interchanged:^{10,11}

$$i\tilde{q}_z + \tilde{q}_{\tau\tau} + 2|\tilde{q}|\tilde{q}^2 = 0. \quad (A2)$$

In Eqs. (A1) and (A2), \tilde{q} represents some property associated with the wave (the field amplitude in the classical theory, or the wave function in the Schrödinger picture for the quantum case). We limit attention to a one-dimensional wave with two independent variables, a “position” ξ (or z) and a “time” t (or τ). Subscripts on \tilde{q} , as usual, correspond to first or second derivatives (one or two subscripts, respectively).

These two types of nonlinear Schrödinger equation are essentially consistent with one another, but (A2) is used in solving boundary value problems, while (A1) is used in initial-value problems.¹⁰ In the classical theory of waves,

these two parabolic equations, which relate to the second approximation of dispersion theory, yield similar soliton solutions which are usually known as fundamental solutions. In some sense, the choice between (A1) and (A2) is a matter of convenience (we have used different independent variables in the two equations). For example, in problems related to the nonlinear diffraction of light, these coordinates are the longitudinal and transverse field distribution. If z and $\tau = t - z/v_g$ (v_g is the group velocity of the wave packet, t is the time) are the space and time (running) propagation coordinates, then Eq. (A2) describes optical solitons.⁵ Their distinctive feature, for example from (A1), is the existence of attraction between second-order solitons (this is the case for two-soliton solutions obtained without the use of perturbation theory for the soliton parameters; see below).^{10,11} Thus, in analyzing Eqs. (A1) and (A2), we are in fact concerned with the interpretation and physical meaning of the independent variables, which depend on the type of problem.

The quantum description of the problem is somewhat different. In quantum mechanics, Eq. (A1) is the Schrödinger equation, which corresponds to the traditional approach in which the derivative with respect to t specifies the temporal evolution of the wave packet, and dynamical processes are described by means of transition probabilities. For optical solitons in spatially distributed systems, it is necessary to go to a boundary-value problem. This is normally based on second quantization of the nonlinear Schrödinger equation (A2), for which the procedure has been analyzed, for example, in Refs. 3, 9, and 12. In the latter case, the particle number operator describes the photon density per unit area.

In the present paper, while taking a general approach to the problems considered, we do no damage to the widely adopted quantum description in which we have the temporal evolution of the state vector (see Eq. 4), but for optical solitons the corresponding variables must be identified [see (9)]. It is also important to note that in perturbation theory, there is no qualitative difference between (A1) and (A2) for two-soliton solutions. In fact, the soliton parameters are then functions of the time t for (A1) and functions of the position z for (A2). As a result, soliton attraction and repulsion become possible in either case. There will, of course, be some quantitative differences, such as in the numerical values of the phase difference [see (27)].

We make brief mention of specifics relating to the production of multisoliton quantum states in the media under consideration. We first consider two-soliton states in one strand of a fiber (see Sec. 3). From a physical standpoint, such solitons can be generated by virtue of the cancellation of dispersion in the medium by phase modulation of the wave a_0 . In the ideal case of noninteracting solitons, the energy of the a_0 field is equally shared by the two solitons. Each is then a fundamental solution only when one takes into account the additional phase shift and spatial translation. In other words, the soliton profiles remain unaltered (see Ref. 7).

In contrast, soliton interactions lead to nontrivial quantum effects (see Sec. 3). In a certain sense, one might say that the two solitons engage in energy exchange. This reduces, however, to just a small redistribution (accessible to

perturbation theory) of the energy of the original field a_0 between the two solitons. Mathematically, this situation is reflected by the fact that two-soliton solutions can be described by the unitary state vector $|\xi_0\rangle$ of the optical wave packet a_0 and by various functions $\Psi_{n_1, n_2}^{(1)}(x, t)$ [see (12) and (23)]. The system can also be described by the unitary Hamiltonian for the 0 mode (cf. Ref. 3).

Physically, the situation is different for coupled solitons in two-strand fibers. Here we have energy exchange between the solitons, which are described by operators a_h and a_0 . In fact, we are dealing with two "types" of bosons, 0 and h , which have "tunneling" interactions in the propagation coordinate and are described by the Hamiltonian (1). The general state vector $|\xi\rangle$ for system of coupled solitons, given by (3), in the approximation we consider here (Hartree), can be represented as a product of the state vectors $|\xi_0\rangle$ and $|\xi_h\rangle$ for each of the solitons [see also (23)],

$$|\xi\rangle|\xi_0\rangle|\xi_h\rangle = \sum_{n,m} \frac{W_{n,m}}{\sqrt{n!m!}} \left\{ \int \Psi_n^{(1)} a_0^+(x) dx \right\}^n \times \left\{ \int \Psi_m^{(2)} a_h^+(x) dx \right\}^m |0\rangle, \quad (A3)$$

where the w_{nm} are given by (5).

Note that energy exchange between the 0 and h solitons should not be "strong," as the coupling constant ε in (11) is fairly small. This is generally the only case in which one can speak of the formation of soliton-like optical wave packets (16) and use perturbation theory for the soliton parameters.

Despite the difference between the physical mechanisms involved in the production of coupled solitons in the two cases considered here, there is some physical analogy in the nature of the interaction in the context of the aforementioned approximations. This in turn makes it possible to more fully understand the behavior of the physical quantities and their fluctuations in nonintegrable systems, which for a variety of reasons would be difficult to analyze directly in the quantum case (for example, due to the operator algebra of those quantities; see Appendix 2).

APPENDIX 2

Quantum nondemolition measurements of the number of photons in a soliton

In this section we detail two types of quantum nondemolition measurements that can be implemented with the aid of interacting solitons.

First, we have the measurement of the number of photons in a signal soliton as a result of its interaction with a probe soliton. A similar problem was considered in Ref. 3, but in contrast to our present approach (based on perturbation theory), the work described in those papers made use of the asymptotic solutions for elastically interacting solitons. Obviously, the number of photons N_i and momenta p_i of the solitons are then conserved quantities. Nevertheless, it was shown that even in this case, ideal quantum nondemolition measurements cannot be implemented automatically.

Mathematically, this comes about because there is no unambiguous relationship between fluctuations in the phase

δ_2 of the probe (measuring) soliton and the number of photons N_1 in the signal (measured) soliton, i.e., there is an additional term responsible for fluctuations in the momentum p_1 of the signal soliton. Only when the state of the soliton is close to a momentum eigenstate can such a term be neglected; that is, only when

$$\langle \Delta p_1^2 \rangle \ll (p_2 - p_1)^2 \frac{\langle \Delta N_1^2 \rangle_{\text{meas}}}{\langle N_1 \rangle^2},$$

where $\langle \Delta N_1^2 \rangle_{\text{meas}}$ is the measurement error for the number of photons in the signal soliton. A similar situation obtains in quantum nondemolition measurements of the position x_1 of a signal soliton.

The physics of the phenomenon is that two-soliton solutions for light result from interaction effects, which not only fail to facilitate quantum nondemolition measurements, but induce additional noise in the measurement process as well.¹⁷ On the other hand, for optical wave packets (solitons, pulsed lasers, cw lasers), similar measurement²⁴ have their own peculiarities, which relate, for example, to the effects of transverse phase modulation (for pulsed and cw lasers), and therefore to changes in wave packet shape. For solitons, this is a manifestation of novel quantum-mechanical characteristics—soliton momenta and positions.

Second, making use of the actual details of soliton interactions, we can in this problem implement a method of making quantum nondemolition measurements of the amplitude difference (number of photons) between the wave packets with the aid of phase difference measurements. We will return to this question in more detail at the end of the present section; for now, we analyze the feasibility of quantum nondemolition measurements of the number of photons and the momentum of the signal soliton during both elastic and inelastic interactions with the probe soliton. Calculations are most convenient for this problem in the Heisenberg picture, wherein the classical Poisson brackets for canonically conjugate quantities become the corresponding commutation relations in the quantum theory of the operators for the parameters in question— η_i (the number of photons), δ_i (the phase), and p_i (the momentum) [see (16)]. These are also solutions of the perturbation problem [see (18) and (21)]. Obviously, in this approach all perturbation calculations [see (16)–(21)] remain valid for the present case as well.

For example, the commutation and uncertainty relations for the number of photons and the phase are

$$[N_i, \delta_j] = i \delta_{ij}, \quad (\text{B1})$$

$$\langle \Delta N_i^2 \rangle \langle \Delta \delta_i^2 \rangle \geq 1/4, \quad i, j = 1, 2. \quad (\text{B2})$$

Further on, however, we will need certain other relations, particularly for the difference in photon numbers and phase for the two solitons:

$$[(N_2 - N_1); (\delta_2 - \delta_1)] = [N_2; \delta_2] + [N_1; \delta_1] = 2i, \quad (\text{B3})$$

$$\langle \Delta(\delta_2 - \delta_1)^2 \rangle \langle \Delta(N_1 - N_2)^2 \rangle \geq 1. \quad (\text{B4})$$

Equation (B4) shows that these differences can be measured for interacting photons as accurately as in the classical theory.

Further calculations based on the specifics of the problem can be conveniently carried out. For example, the quantities $\eta_{1,2}$ and $p_{1,2}$ individually are not constants of the motion in the present problem, but there is such a constant of the motion (20) for their differences $\delta p \equiv p_2 - p_1$ and $\delta \eta \equiv \eta_2 - \eta_1$. Starting with this information, let us calculate fluctuations in the phase difference and the intersoliton distance. To do so, we make use of the techniques described in Ref. 3.

In the semiclassical limit, the operators can be put in the form

$$\begin{aligned} \eta_i &= \eta_{i,c} + \Delta \eta_i, & \delta_i &= \delta_{i,c} + \Delta \delta_i, & \tau_i &= \tau_{i,c} + \Delta \tau_i, \\ p_i &= p_{i,c} + \Delta p_i, & i &= 1, 2, \end{aligned} \quad (\text{B5})$$

where $\eta_{i,c}$, $\delta_{i,c}$, $\tau_{i,c}$, and $p_{i,c}$ are the regular (coherent) classical parts, and $\Delta \eta_i$, $\Delta \delta_i$, $\Delta \tau_i$, and Δp_i are operators, where these operator increments (i.e., their eigenvalues) are assumed small—for example, $\Delta \eta_i \ll \eta_{i,c}$ (for brevity, we omit any special notation from operators). We then have

$$\begin{aligned} \langle \eta_i \rangle &= \eta_{i,c}, & \langle \Delta \eta_i \rangle &= 0, \\ \langle \delta_i \rangle &= \delta_{i,c}, & \langle \Delta \delta_i \rangle &= 0, \\ \langle \tau_i \rangle &= \tau_{i,c}, & \langle \Delta \tau_i \rangle &= 0, \\ \langle p_i \rangle &= p_{i,c}, & \langle \Delta p_i \rangle &= 0. \end{aligned} \quad (\text{B6})$$

We can write similar relations for φ , $\delta \eta$, r , and δp .

In the semiclassical limit, we have for the fluctuations in the intersoliton phase difference and distance operators $\Delta \varphi$ and Δr (see Ref. 3)

$$\begin{aligned} \Delta \varphi(t) &= \frac{\partial \varphi_0(t)}{\partial \eta} \Delta \eta + \frac{\partial \varphi(t)}{\partial r_0} \Delta r_0 + \frac{\partial \varphi(t)}{\partial p} \Delta p \\ &+ \frac{\partial \varphi(t)}{\partial \varphi_0} \Delta \varphi_0 + \frac{\partial \varphi(t)}{\partial(\delta p_0)} \Delta(\delta p_0) \\ &+ \frac{\partial \varphi(t)}{\partial(\delta \eta_0)} \Delta(\delta \eta_0), \end{aligned} \quad (\text{B7})$$

$$\begin{aligned} \Delta r(t) &= \frac{\partial r(t)}{\partial \eta} \Delta \eta + \frac{\partial r(t)}{\partial r_0} \Delta r_0 + \frac{\partial r(t)}{\partial p} \Delta p + \frac{\partial r(t)}{\partial \varphi_0} \Delta \varphi_0 \\ &+ \frac{\partial r(t)}{\partial(\delta p_0)} \Delta(\delta p_0) + \frac{\partial r(t)}{\partial(\delta \eta_0)} \Delta(\delta \eta_0), \end{aligned} \quad (\text{B8})$$

where $\varphi_0 \equiv \varphi(t=0)$, $r_0 \equiv r(t=0)$, $\delta p_0 \equiv \delta p(t=0)$, and $\delta \eta_0 \equiv \delta \eta(t=0)$ are the values of these quantities at time $t=0$.

Equations (B7) and (B8) for two interacting solitons take account of interference between the noise sources associated with each, so one can only speak of their joint effects on fluctuations. This distinguishes our approach from the treatment given in Ref. 3, where the contribution of each soliton to the difference in fluctuations $\langle \Delta r^2(t) \rangle$ or $\langle \Delta \varphi^2(t) \rangle$ was identified. Analysis of (B7) and (B8) is difficult in the general case, so we assume that $\delta p_0 = 0$, $\delta \eta_0 = 0$, $\mu = 0$, i.e., $\psi(0) = 0$ [see (27)], corresponding to the oscillatory mode of soliton interaction:

$$\Delta r(t) = \frac{\partial r(t)}{\partial \eta} \Delta \eta + \frac{\partial r(t)}{\partial r_0} \Delta r_0 - 2t \Delta(\delta p_0), \quad (\text{B9})$$

where

$$\begin{aligned} \frac{\partial r(t)}{\partial \eta} &= \frac{1}{2\eta_c} \left\{ -\frac{1}{\eta_c} \ln \left[\frac{1}{2} (1 + \cos(4\eta_c \nu t)) \right] \right. \\ &\quad \left. - \frac{4t(2 - \eta_c r_0) \nu \sin(4\eta_c \nu t)}{1 + \cos(4\eta_c \nu t)} \right\}, \\ \frac{\partial r(t)}{\partial r_0} &= 1 + 2t\eta_c \nu \frac{\sin(4\eta_c \nu t)}{1 + \cos(4\eta_c \nu t)}, \\ \frac{\partial \varphi(t)}{\partial \eta} &= -2p \frac{\partial r(t)}{\partial n}, \\ \frac{\partial \varphi}{\partial p} &= -\{ -4\eta_c t r_0 \nu \operatorname{tg}(2\eta_c \nu t) + 2(r_c(t) - r_c(0)) \}, \\ \frac{\partial \varphi}{\partial r_0} &= -\left\{ -4\eta_c t \nu p_c \operatorname{tg}(2\eta_c \nu t) + 2p \left(\frac{\partial r(t)}{\partial r_0} - 1 \right) \right\}, \\ \frac{\partial \varphi}{\partial \varphi_0} &= 1 + 2\eta_c \nu t \operatorname{tg}(2\eta_c \nu t), \\ \frac{\partial \varphi}{\partial(\delta \eta_0)} &= 4\eta_c t, \quad \frac{\partial \varphi}{\partial(\delta p)} = 4p_c t. \end{aligned} \quad (\text{B10})$$

Even with the assumptions made above, it is clear from (B9) and (B10) that there is a nonvanishing contribution to the fluctuations $\Delta r(t)$ due to the terms $\partial r/\partial n$ and $\partial r/\partial(\delta p_0)$, with similar considerations for the fluctuations $\Delta \varphi$.

We consider the special case in which $4\eta_c \nu t = 2\pi$, i.e., we are only interested in the behavior of fluctuations over a time corresponding to the oscillation period T_{osc} [see (30)]. Then both the distance between solitons and their phase difference are constants of the motion [as are the number of photons and momentum of each soliton taken individually; see (31)], so from (B9) and (B10) we have

$$\Delta r(t) = \Delta r_0 - 2t \Delta(\delta p_0), \quad (\text{B11})$$

$$\Delta \varphi(t) = \Delta \varphi_0 + 4\eta_c t \Delta(\delta \eta_0) + 4p_c t \Delta(\delta p_0). \quad (\text{B12})$$

This approximation corresponds to the elastic limit of soliton interaction. Hence, we have for the mean squared fluctuations

$$\langle \Delta r^2(t) \rangle = \langle \Delta r_0^2 \rangle + 4t^2 \langle \Delta(\delta p_0)^2 \rangle, \quad (\text{B13})$$

$$\langle \Delta \varphi^2(t) \rangle = \langle \Delta \varphi_0^2 \rangle + 16\eta_c^2 t^2 \langle \Delta(\delta \eta_0)^2 \rangle + 16p_c^2 t^2 \langle \Delta(\delta p_0)^2 \rangle, \quad (\text{B14})$$

where we have assumed all fluctuations to be initially independent. The measurement errors in the amplitude and momentum differences between the two solitons can then be estimated to be

$$\langle \Delta r^2(t) \rangle \geq 4t^2 \langle \Delta(\delta p_0)^2 \rangle, \quad (\text{B15})$$

$$\langle \Delta \varphi^2(t) \rangle \geq 16\eta_c^2 t^2 \langle \Delta(\delta \eta_0)^2 \rangle + 16p_c^2 t^2 \langle \Delta(\delta p_0)^2 \rangle. \quad (\text{B16})$$

Further, in the interests of brevity, we calculate the number of photons only for quantum nondemolition measurements. Noting that $(\eta_{1,2})_c \propto n_{1,2}$ [see (17)], we obtain

$$\langle \Delta(\delta \eta_0)^2 \rangle = \frac{\kappa^2}{16} (\langle \Delta \eta_2^2 \rangle + \langle \Delta \eta_1^2 \rangle). \quad (\text{B17})$$

Our final result is therefore

$$\begin{aligned} \langle \Delta \delta_1^2(t) \rangle + \langle \Delta \delta_2^2(t) \rangle &\geq 16\eta_c^2 t^2 (\langle \Delta \eta_1^2 \rangle_{\text{meas}} + \langle \Delta \eta_2^2 \rangle) \\ &\quad + 16p_c^2 t^2 (\langle \Delta p_1^2 \rangle + \langle \Delta p_2^2 \rangle). \end{aligned} \quad (\text{B18})$$

This yields our conclusion.

To obtain quantum nondemolition measurements of the number of photons n_1 in the signal soliton, it is necessary that [see (B17)]

$$\begin{aligned} \langle \Delta \delta_1^2 \rangle &\geq 16\eta_c^2 t^2 \langle \Delta \eta_2^2 \rangle + 16p_c^2 t^2 \langle \Delta p_2^2 \rangle \\ \langle \Delta \delta_2^2 \rangle &\geq 16\eta_c^2 t^2 \langle \Delta \eta_1^2 \rangle_{\text{meas}} + 16p_c^2 t^2 \langle \Delta p_1^2 \rangle. \end{aligned} \quad (\text{B19})$$

The latter equation for $\langle \Delta \delta_2^2 \rangle$ shows that we are dealing with nonideal quantum nondemolition measurements, since there is an additional source of noise associated with momentum fluctuations $\langle \Delta p_1^2 \rangle$. Nevertheless, satisfaction of (B19) implies the validity of (B18) as well. Note that the converse is not always true, since phase fluctuations of the probe field can also result from fluctuations in the number of photons, as occurs when self-interaction effects develop. Based on (B18), it would therefore be more correct to be discussing the feasibility of stabilizing the noise (phase or photon numbers) of two coupled solitons. On the other hand, this kind of stabilization is also possible through quantum nondemolition measurements of the number of photons in the signal soliton (see, for example, Refs. 3 and 17).

In order for quantum nondemolition measurements to be of high quality (close to ideal), we must have

$$\langle \Delta p_1^2 \rangle \ll \frac{\eta_c^2}{p_c^2} \langle \Delta \eta_1^2 \rangle_{\text{meas}}, \quad (\text{B20})$$

which is easily derived from (B19), i.e., the signal soliton needs to be approximately in a momentum eigenstate (see Ref. 3). The better the fluctuations are suppressed, the closer we are to ideal quantum nondemolition measurements. These fluctuations can in principle be brought to a level lower than their vacuum value, for instance by increasing fluctuations in the conjugate quantity, the soliton position (as is usually done in generating quadrature squeezed light).

Finally, we note that in the other limiting case [as in the derivation of (B9) and (B10)], in which the distance between solitons grows ($\nu=0$), actual calculations [based on Eqs. (21), (22), (B7), and (B8)] show that quantum nondemolition measurements retreat farther from the ideal.

We now briefly examine the feasibility of implementing quantum nondemolition measurements of the difference in soliton photon numbers via measurements of their phase differences. Mathematically, this statement of the problem is better grounded than the approach taken above.

In fact, in treating interacting solitons, we obtained a relationship between their phase differences, amplitudes, positions, and momenta [see (21)]. To assess the feasibility of implementing qualitatively similar high-precision measurements, it is convenient to introduce two correlation coefficients (see Refs. 24, 27):

$$K_1 = \frac{|\langle \delta\eta(0)\delta\eta(t) \rangle + \langle \delta\eta(t)\delta\eta(0) \rangle - 2\langle \delta\eta(0) \rangle \langle \delta\eta(t) \rangle|^2}{4\langle (\Delta(\delta\eta(0)))^2 \rangle \langle (\Delta(\delta\eta(t)))^2 \rangle}, \quad (B21)$$

$$K_2 = \frac{|\langle \delta\eta(0)\varphi(t) \rangle + \langle \varphi(t)\delta\eta(0) \rangle - 2\langle \delta\eta(0) \rangle \langle \varphi(t) \rangle|^2}{4\langle (\Delta(\delta\eta(0)))^2 \rangle \langle (\Delta(\varphi(t)))^2 \rangle}. \quad (B22)$$

Here K_1 specifies the correlation between the measured difference in amplitude (photon numbers) at times $t=0$ and t , and it characterizes the degree to which the measured quantity [in this case $\delta\eta(0)$] is conserved. K_2 indicates how accurately such a measurement can be made in terms of the phase difference in $\varphi(t)$. For ideal quantum nondemolition measurements, we have

$$\delta\eta(0) = \delta\eta(t), \quad K_1 = 1, \quad (B23)$$

$$\delta\varphi(t) = \lambda \delta\eta(0), \quad K_2 = 1, \quad (B24)$$

where λ is a numerical factor associated with the measurement process itself. Analysis of the final Eqs. (21) (in the Heisenberg picture) shows that in general, implementation of quantum nondemolition measurements of the difference in photon numbers is far from an ideal case. In the semiclassical approximation that we have considered (with $\mu=0$, $4\eta_c \nu t = 2\pi$, and $\delta\eta_c \approx \delta p_c \approx 0$), it is clear from Eq. (B12) that $\Delta\varphi(t) \sim \Delta(\delta\eta_0)$ (the latter term, which is associated with fluctuations in δp_0 , reflects the nonideal nature of the quantum nondemolition measurements). Accordingly, $\delta\eta_0(t) \approx \delta\eta_0(0)$.

Note that similar coefficients can also be introduced to measure the soliton momentum difference $\delta p(0)$ by measuring the position difference. We must then make the replacements $\delta\eta \rightarrow \delta p$ and $\varphi \rightarrow r$ in (B21) and (B22).

Thus, we see from the foregoing discussion that over a period T_{osc} it becomes possible in principle to conduct quantum nondemolition measurements of the difference in soliton photon numbers [$\delta\eta(t) \sim N_2 - N_1$] by making use of their phase differences (see Ref. 25). A more detailed and convincing discussion of the practical implementation of such measurements in an actual experiment would require considerable further discussion, which lies beyond the scope of the present paper. Here we merely note that the present analysis hints at the high quality of such measurements in the polarization characteristics (for the Stokes parameters) of a light signal.²⁸

In closing, let us compare the two approaches to quantum nondemolition measurements that we have proposed. The major difference would appear to be that in the first case, where we deal with the number of photons in the signal soliton, high-precision measurements can in principle only take place over the oscillation period T_{osc} . Undesirable self-interaction effects can then be suppressed by special means.¹⁸ In the second case, such measurements (with other than the parameter values adopted above) lose meaning, since in practical terms they are made under conditions that are far from ideal [by virtue of the functional terms in Eq. (21)].

- ¹M. Wadati, A. Kumiba, and T. Konishi, *J. Phys. Soc. Jpn.* **54**, 1710 (1985); B. Yoon and J. W. Negele, *Phys. Rev. A* **16**, 1451 (1977).
- ²B. Yurke and H. Y. Potasek, *J. Opt. Soc. Am.* **6**, 1227 (1989).
- ³H. A. Haus, R. Watanabe, and Y. Yamamoto, *J. Opt. Soc. Am.* **6**, 1138 (1989); Y. Lai and H. A. Haus, *Phys. Rev. A* **40**, 844 (1989); Y. Lai and H. A. Haus, *Phys. Rev. A* **40**, 854 (1989).
- ⁴A. S. Chirkin and A. V. Belinskii, *Zh. Éksp. Teor. Fiz.* **98**, 407 (1990) [*Sov. Phys. JETP* **71**, 228 (1990)]; A. V. Belinskii, *Zh. Éksp. Teor. Fiz.* **103**, 1914 (1993) [*Sov. Phys. JETP* **76**, 947 (1993)].
- ⁵F. Kh. Abdullaev, S. A. Darmanyan, and P. K. Khabibullaev, *Optical Solitons*, Springer-Verlag, New York (1993), Ch. VIII; S. A. Darmanyan, *Zh. Tekh. Fiz.* **61**, No. 11, 217 (1991) [*Sov. Phys. Tech. Phys.* **36**, 1321 (1991)].
- ⁶P. N. Elyutin, *Usp. Fiz. Nauk* **155**, 397 (1988) [*Sov. Phys. Usp.* **31**, 597 (1988)].
- ⁷V. E. Zakharov and A. B. Shabat, *Zh. Éksp. Teor. Fiz.* **61**, 118 (1971) [*Sov. Phys. JETP* **34**, 62 (1971)].
- ⁸V. I. Karpman and E. M. Maslov, *Zh. Éksp. Teor. Fiz.* **73**, 537 (1977) [*Sov. Phys. JETP* **46**, 281 (1977)].
- ⁹A. P. Alodzhants and S. M. Arakelyan, *Zh. Éksp. Teor. Fiz.* **103**, 910 (1993) [*JETP* **76**, 445 (1993)].
- ¹⁰T. Yajima and M. Wadati, *J. Phys. Soc. Jpn.* **59**, 3237 (1990).
- ¹¹S. A. Darmanyan and V. J. Rupasov, in *Future Directions of Nonlinear Dynamics in Physical and Biological Systems*, P. Christiansen, J. Eilbeck, and R. Parmentiers (eds.), Plenum, New York (1993), p. 101.
- ¹²M. D. Levenson, R. M. Shelby, M. Reid, and D. F. Walls, *Phys. Rev. Lett.* **57**, 2473 (1986).
- ¹³A. A. Maier, *Kvant. Elektron.* **11**, 157 (1984) [*Sov. J. Quantum Electron.* **14**, 101 (1984)].
- ¹⁴V. S. Afraimovich, in *Nonlinear Waves: Structure and Bifurcations* [in Russian], A. V. Gaponov-Grekhov and M. I. Rabinovich (eds.), Nauka, Moscow (1987); F. M. Zaslavskii and R. Z. Sagdeev, *Introduction to Nonlinear Physics: From the Pendulum to Turbulence and Chaos* [in Russian], Nauka, Moscow (1988); F. M. Zaslavskii, R. Z. Sagdeev, D. A. Ushakov, and A. A. Chernikov, in: *Nonlinear Waves: Dynamics and Evolution* [in Russian], A. V. Gaponov-Grekhov and M. I. Rabinovich (eds.), Nauka, Moscow (1989), p. 84.
- ¹⁵A. V. Belinskii and A. S. Chirkin, *Kvant. Elektron.* **15**, 873 (1988) [*Sov. J. Quantum Electron.* **18**, 560 (1988)].
- ¹⁶D. F. Smimov and A. S. Troshin, *Usp. Fiz. Nauk* **153**, 233 (1987) [*Sov. Phys. Usp.* **30**, 851 (1987)]; M. C. Teich and B. E. A. Saleh, *Usp. Fiz. Nauk* **161**, 101 (1991).
- ¹⁷Y. Yamamoto and H. A. Haus, *Rev. Mod. Phys.* **58**, 1001 (1986); N. Imoto, H. A. Haus, and Y. Yamamoto, *Phys. Rev. A* **33**, 2287 (1985).
- ¹⁸Yu. I. Vorontsov, *Usp. Fiz. Nauk* **164**, No. 1, 89 (1994); V. B. Braginskii (Braginsky) and F. Ya. Khalili, *Rev. Mod. Phys.* (1995), in press.
- ¹⁹S. Weigert, *Phys. Rev. A* **43**, 6597 (1991).
- ²⁰V. P. Bykov, *Usp. Fiz. Nauk* **161**, 145 (1991) [*Sov. Phys. Usp.* **34**, 417 (1991)].
- ²¹B. V. Chirikov, "The uncertainty principle and quantum chaos," Second Int. Workshop on Squeezed States and Uncertainty Relations, May 25–29, 1992, Moscow, in *NASA Conf. Pub.*, D. Han, Y. S. Kim, and V. I. Mak'ko (eds.), Goddard Space Flight Center, Greenbelt, Maryland (1993), p. 317; B. V. Chirikov, *Chaos* **1**, 95 (1991).
- ²²A. Peres, "Quantum chaos and the measurement problem," in *Quantum Measurement and Chaos*, E. R. Pike and S. S. Sarkar (eds.), NATO ASI Series, Ser. B, Physics, Vol. 161, Plenum, New York (1987), p. 59.
- ²³A. P. Alodzhants (Alodjants), S. M. Arakelyan (Arakelian), and Yu. S. Chilingaryan (Chilingarian), *Laser Physics* **2**, 341 (1992).
- ²⁴S. M. Arakelyan, *Kvant. Elektron.* **20**, 969 (1993) [*Sov. J. Quantum Electron.* **23**, 843 (1993)]; A. P. Alodzhants (Alodjants) and S. M. Arakelyan (Arakelian), *Laser Physics* **4**, 765 (1994).
- ²⁵C. Fabre, E. Giacobino, A. Heidmann *et al.*, *Quant. Opt.* **2**, 159 (1990).
- ²⁶V. K. Ignatovich, "Classical interpretation of quantum mechanics" [in Russian], Joint Institute of Nuclear Research, Dubna, Rep. No. R4-92-389 (1992); Yu. I. Zaporovannyi, V. V. Kuryshkin, and I. A. Lyabis, *Izv. Vyssh. Uchebn. Zaved., Fiz. No. 3*, 80 (1978).
- ²⁷A. N. Chaba, M. Y. Collet, and D. F. Walls, *Quant. Opt.* **4**, 119 (1992).

²⁸ A. P. Alodzhants, S. M. Arakelyan, and A. S. Chirkin, Zh. Éksp. Teor. Fiz. **107**, 7 (1995) [JETP **81**, 7 (1995)].

Note added in proof (May 10, 1995): The analysis presented here of the solutions of the coupled nonlinear quantum Schroedinger equations can also be useful for studying atomic solitons [G. Lenz, P. Meystre, and E. M.

Wright, Phys. Rev. A **50**, 1681 (1994)]. In this case the nonlinearity results from interference of N bosonlike two-level atoms, while the linear coupling between the wave functions is due to the interaction of the atoms with the standing wave of the classical laser field.

Translated by Marc Damashek